UNIVERSITY OF KWAZULU-NATAL
INYUVESI YAKWAZULU-NATALI

New Dithiophosphonate Complexes of Nickel, Cadmium, Mercury and Lead

by

Shirveen Sewpersad

Dissertation submitted in fulfilment of the academic requirements for the degree of

Master of Science

School of Chemistry and Physics, University of KwaZulu-Natal, Durban

January 2013

Declaration 1: Plagiarism

I, Shirveen Sewpersad, declare that the experimental work described in this dissertation was carried out at the School of Chemistry and Physics, University of KwaZulu-Natal, Westville campus, between March 2011 and November 2012, under the supervision of Dr. W.E. van Zyl, and Dr. P.G. Ndungu and that:

1. The research reported in this thesis, except where otherwise indicated, is my original research.
2. This thesis has not been submitted for any degree or examination at any other university.
3. This thesis does not contain other persons' data, pictures, graphs or other information, unless specifically acknowledged as being sourced from other persons.
4. This thesis does not contain other persons' writing, unless specifically acknowledged as being sourced from other researchers. Where other written sources have been quoted, then:
    a. Their words have been re-written but the general information attributed to them has been referenced
    b. Where their exact words have been used, then their writing has been placed in italics and inside quotation marks, and referenced.
5. This thesis does not contain text, graphics or tables copied and pasted from the Internet, unless specifically acknowledged, and the source being detailed in the thesis and in the References sections.

Signed

_____

Shirveen Sewpersad

Declaration 2 : Publications

Details of publications:

1. S. Sewpersad, B. Omondi and W. E. Van Zyl, *Acta Crystallographica Section E*, 2012, **68**, m1483.
2. S. Sewpersad and W. E. Van Zyl, *Acta Crystallographica Section E*, 2012, **68**, m1457.
3. S. Sewpersad, B. Omondi and W. E. Van Zyl, *Acta Crystallographica Section E*, 2012, **68**, m1534.
4. S. Sewpersad and W. E. Van Zyl, *Acta Crystallographica Section E*, 2012, **68**, m1488-m1489.
5. S. Sewpersad and W. E. Van Zyl, *Acta Crystallographica Section E*, 2012, **68**, m1502.

From all the above publications, my role included carrying out all the experimental work and contributing to the writing of the publications along with my supervisor. The other co-author's contribution was that of an editorial nature and checking on the scientific content and evaluation of my interpretation and based on his expertise, he has added minor parts to the papers above.

Signed

_____

Shirveen Sewpersad

Abstract

This study was primarily focused on the synthesis and structural X-ray crystallographic analyses of new complexes. The work undertaken investigated the reactivity of the diphosphetane disulfide dimer, $[P(4\text{-}C_6H_4OEt)S(S)]_2$, which is the phenetole analogue of the popular Lawesson's Reagent (LR), towards the primary and secondary alcohols methanol, 2-propanol, 1-propanol and 2-butanol. The phenetole LR dimer undergoes nucleophilic attack when reacted with primary or secondary alcohol species, cleaving it symmetrically and forming the respective dithiophosphonic acid, which is then readily deprotonated by ammonia, yielding ammonium dithiophosphonato ligand salts of the type $NH_4[S_2PR(OR')]$ ($R=4\text{-}C_6H_4OEt$) used directly in complexing metals centres. The dithiophosphonato ligands are all bidentate and mono-anionic. New late transition-metal complexes were formed from the reaction between $[S_2PR(OR')]^-$ with the halide or nitrate salts of Cadmium(II), Nickel(II), Lead(II) and Mercury(II), affording both mononuclear and dinuclear complexes. Suitable crystals of nine complexes were eventually found and subjected to X-ray crystallographic analyses: four distorted square planar Ni(II) complexes (**1A, 2A, 3A, 4A**), two dinuclear Hg(II) complexes (**1B, 2B**), one dinuclear Cd(II) complex (**1C**) and one distorted pyramidal dimeric Pb(II) complex (**2D**) and an octahedral Ni(II) complex (**4Ai**). Additionally, all new complexes were fully characterized by means of ^{31}P and ^{1}H and ^{13}C NMR, FTIR, elemental analysis and, as stated, single crystal X-Ray diffraction. This study initially set out to determine if small changes in starting materials could lead to significant changes in structure (as it often does, through unexpected hydrogen bonding, for example), but it turned out in this study that most of the complexes prepared, although new, did not deviate significantly from the structural details of related complexes previously prepared, which is a result in itself.

To my family, in memory of my Dad

If *by Rudyard Kipling*

If you can keep your head, when all about you
are losing theirs and blaming you,
If you can trust yourself when all men doubt you,
But make allowance for their doubting too,
If you can wait and not be tired by waiting,
Or being lied about don't deal in lies
Or being hated don't give way to hating
and yet not look too good nor talk too wise

If you can dream and not make dreams your master
If you can think and not make thoughts your aim
If you can meet with triumph and disaster
And treat those two imposters just the same
If you can watch the truth you've spoken
Twisted by knaves To make a trap for fools
Or watch the things you gave your life too, broken
And stoop and build 'em up with worn out tools

If you can make one heap of all your winnings
And risk it on one turn of pitch and toss
And lose and start again at you beginnings,
And never breathe a word about your loss
If you can force your heart and nerve and sinew
To serve you long after they are gone, and
So hold on when there is nothing in you
Except the will which says to them-Hold On
If you can talk with crowds and keep your virtue
Or walk with kings nor lose the common touch
If neither foe, nor loving friend can hurt you
If all men count with you, but none too much
If you can fill the unforgiving minute with sixty seconds worth of distance run
Then yours is the Earth and everything that's in it
and...which is more...you'll be a man my son!

Acknowledgements

My family, without your love, support and sacrifice, nothing would be possible.

My supervisors Dr. W.E. van Zyl and Dr. P.G. Ndungu for giving me the opportunity and guidance throughout this study.

Dr. Hong Su, Dr. B.O. Owaga and Mr. S. Zamisa for collection and refinement of all X-Ray crystallographic data contained in this dissertation.

The technical and support staff of the School of Chemistry and Physics at UKZN Westville, who always had time for my requests, however big or small.

My campus family Kaalin Gopaul, Vashen Moodley, Michael Pillay, Fezile Potwana and Sicelo Sithole for their patience and support, you guys made every day a good one.

My friends Kyle Gaffar, Rishab Goonoa, Kavashen Naidoo, Samashen Pillay, Ashvir 'Pods' Ramowtar, Preshendra Sewsunker, Kamal Singh and last but not least Sasha Sankar, for being there.

The Catalysis Research Group for giving me a change of scenery when I needed it.

Finally to the National Research Foundation for a generous Innovation Grant which provided invaluable assistance throughout this study.

Abbreviations and Symbols

^{o}C	degrees Celsius
Å	Angstrom
MHz	mega Hertz
cm^{-1}	wavenumbers
λ	wavelength
ppm	parts per million
DCM	dichloromethane (CH_2Cl_2)
tptz	2,4,6-tris(2-pyridyl)-1,3,5-triazine
tbp	4-tertbutyl pyridine
$CDCl_3$	deuterated chloroform
NMR	Nuclear Magnetic Resonance
• ^{1}H	Proton Nuclei
• ^{13}C	Carbon-13 Nuclei
• ^{31}P	Phosphorus-31 Nuclei
• s	singlet
• d	doublet
• t	triplet
• quart	quartet
• dd	doublet of doublets
• d quart	doublet of quartets
• m	multiplet
FTIR	Fourier Transform Infrared
IR	Infrared
• s	strong
• m	medium
• w	weak
IUPAC	International Union of Pure and Applied Chemistry
PIN	Preferred IUPAC name
HSAB	Hard and Soft acid-base
ORTEP	Oak Ridge thermal ellipsoid plot

Table of Contents

List of Figures

List of Schemes

List of Tables

Chapter 1 : Introduction

Dithio-organophosphorus compounds have a history of being used as ligands in inorganic chemistry. Studies based on the use of these compounds have provided inorganic chemists with novel ligand classes affording unique metal co-ordination geometries, thereby providing building blocks for further research into avenues such as metal organic frameworks and other supramolecular studies.[1] The phosphor-1,1-dithiolato ligands are an important example of dithio-organophosphorus compounds reported in such research and provide the basis for the present study. Lawesson's reagent and its precursor phosphorus pentasulfide (Berzelius reagent), have both proven important starting materials in the synthesis of phosphor-1,1-dithiolato ligands.[2, 3]

1.1 Lawesson's reagent

Lawesson's reagent and its analogues (**Figure 1.1**) are all cyclic dimers commonly known as diphosphetane disulfides.[4] This class of compounds was first reported in 1952 by Fay and Lankelma,[5] who investigated the reaction of cyclohexene with phosphorus pentasulfide (P_4S_{10}), forming a dimer (**A**). The synthetic procedure and characterization of dimer **A,** however, was not reported until 1962 by Newallis *et al.*[6] This synthetic procedure entailed bubbling H_2S gas into $PhP(S)Cl_2$ at a temperature of 210 °C which resulted in the formation of the desired product along with copious amounts of corrosive HCl as a by-product**,** shown in **Scheme 1.1**.

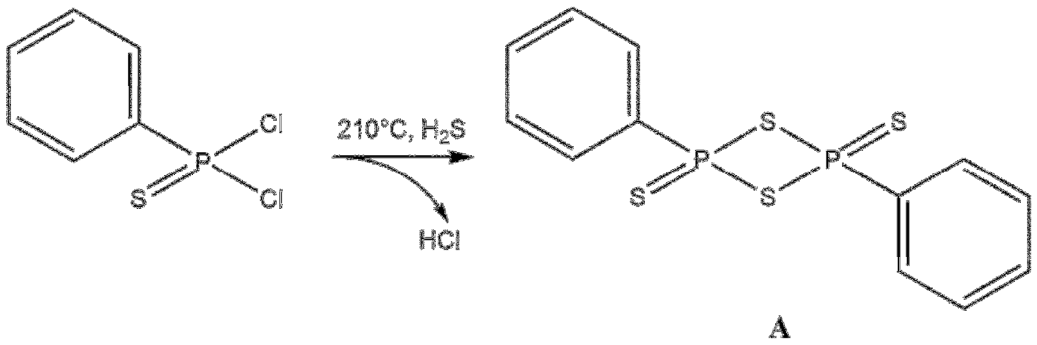

A

Scheme 1.1: Reaction scheme for the synthesis of dimer A

This method has been succeeded by the far less hazardous and far more facile reaction of phosphorus pentasulfide (P_4S_{10}) with electron rich aromatics. Lawesson's reagent (**B**) and its phenetole analogue (**C**) are both readily prepared by the reflux of P_4S_{10} in either anisole or phenetole (**Scheme 1.2**), respectively. The synthesis of a ferrocenyl derivative (**D**) requires the reflux of P_4S_{10} in a suspension of ferrocene and xylene, this ferrocenyl Lawesson's reagent (FcLR) was first reported by Woollins and co-workers, and was of great interest due to the incorporation of an organometallic moiety into the ligand.[7] Woollins and co-workers also reported the formation of a selenium analogue (**E**) now commercially available as Woollins' Reagent, which has gained widespread use as a selenation reagent.[8-13] A study into the synthesis and use of fluorous derivatives of Lawesson's reagent has been made by Dembinski and co-workers in 2006 **(F)**.[14] The primary step in the study was the addition of a fluorous 'ponytail' to the anisole group. This study also showed how, through use of methylene spacer groups, the electron withdrawing effects of fluorinating the anisole could be negated, thus maintaining the electron rich nature of the aromatic, required for the subsequent reaction with P_4S_{10}.[14]

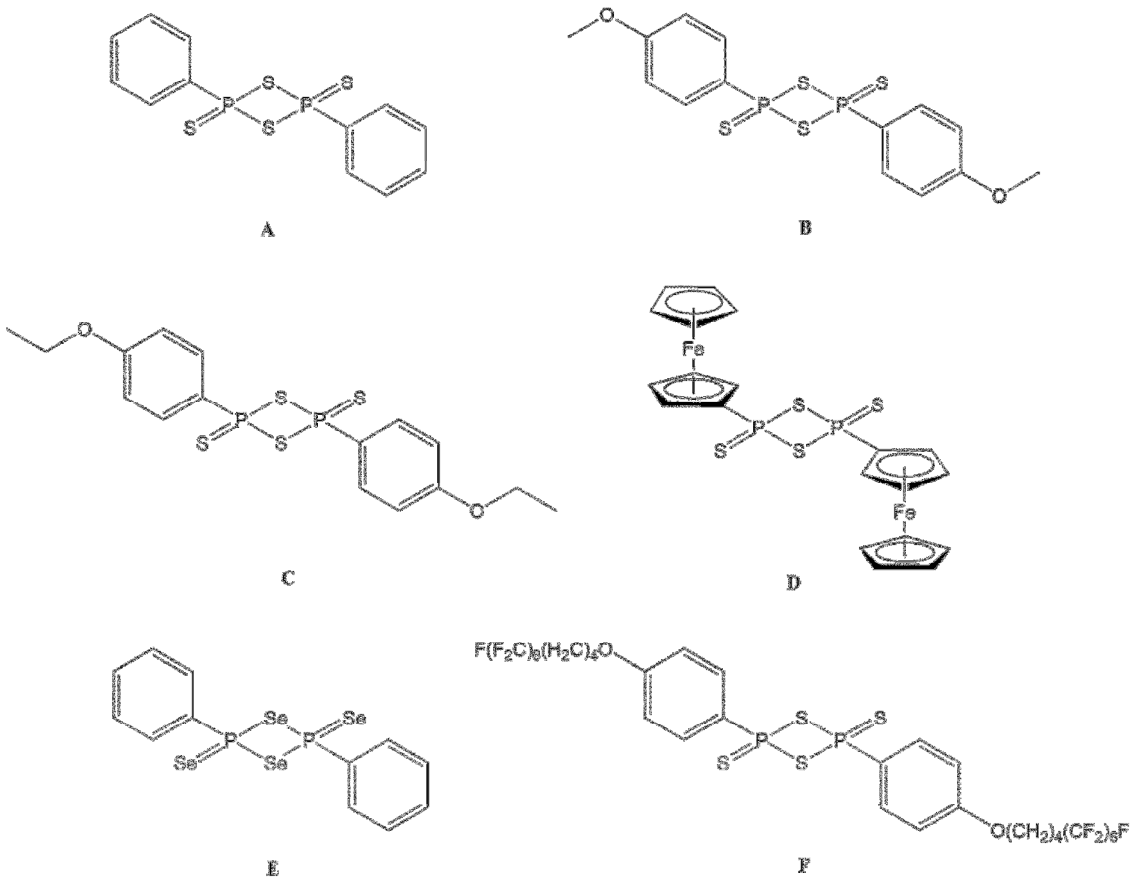

Figure 1.1: A comparative representation of diphosphetane disulfide dimers

Lawesson's reagent has a long history of being applied as a thionating agent in organic chemistry, but only relatively recently have the dithiophosphonate class ligands, borne from the reaction of LR with alcohols, been investigated in co-ordination chemistry with transition metals.[3]

1.2 Phosphor-1,1-dithiolato ligands

This class of compounds is characterised by having the S_2P functionality and is subdivided broadly into three distinct subclasses: the dithiophosphates, dithiophosphinates and the dithiophosphonates. It is important to note that systematic nomenclature is cumbersome when referring to compounds in this class and thus usually avoided in preference for IUPAC

names. In the case of phosphor-1,1-dithiolato ligands, two naming systems are frequently used in literature. The preferred IUPAC name (PIN) for phosphor-1,1-dithiolato compounds are phosphorodithioates, phosphonodithioates and phosphinodithioates which correspond to the commonly used dithiophosphates (**G**), dithiophosphonates (**H**) and dithiophosphinates (**I**), respectively, for the same compounds. The latter naming system has been used consistently throughout the present study.

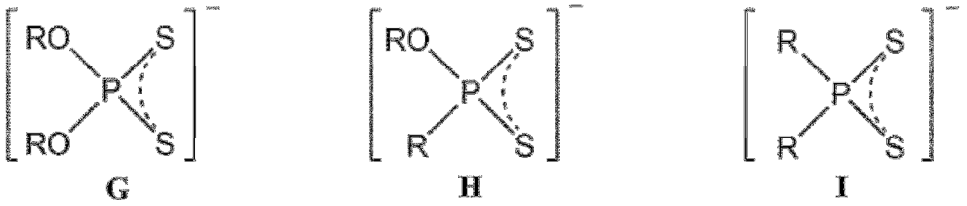

Figure 1.2: Ligand classes: (G) Dithiophosphato ; (H) Dithiophosphonato ; (I) Dithiophosphinato

The chemistry of the dithiophosphate and dithiophosphinate subclasses has been well developed, with complexes of main group- and transition-metals being far more abundant in literature than those of the dithiophosphonates,[15, 16] probably due to the greater challenges represented in the synthesis of ligands in the latter subclass, and their subsequent commercial unavailability and sensitivity towards hydrolysis.[2] The symmetrical nature of dithiophosphate and dithiophosphinate-based ligands both afford no isomeric variance when reacted with transition metals, whereas the 'hybrid' dithiophosphonates are uniquely non-symmetric, thereby affording the possibility of adopting more complex isomers when reacting with similar transition metals.

Dithiophosphonic acids [H{S_2PR(OR')}] are readily synthesized by the symmetric cleavage of diphosphetane disulfide dimers, such as Lawesson's reagent [(4-$MeOC_6H_4P(S)S)_2$] or its phenetole analogue [(4-$EtOC_6H_4P(S)S)_2$], by two stoichiometric equivalents of primary or

secondary alcohol. Similarly attempted reactions with tertiary alcohols have been shown to result in an elimination reaction rather than the formation of the desired dithiophosphonic acid.[3] Deprotonation of the acid by a weak base such as ammonia yields the dithiophosphonate salt $NH_4[S_2PR(OR')]$.

A variation of this procedure using sodium alkoxide salts to circumvent the use of ammonia has been reported.[17] Variation in the alcohol as well as the phosphetane dimer used offers a wide scope for investigation into a multitude of new dithiophosphonate derivatives, and selective variation of either reactant delivers control in ligand design with respect to steric and electronic properties.

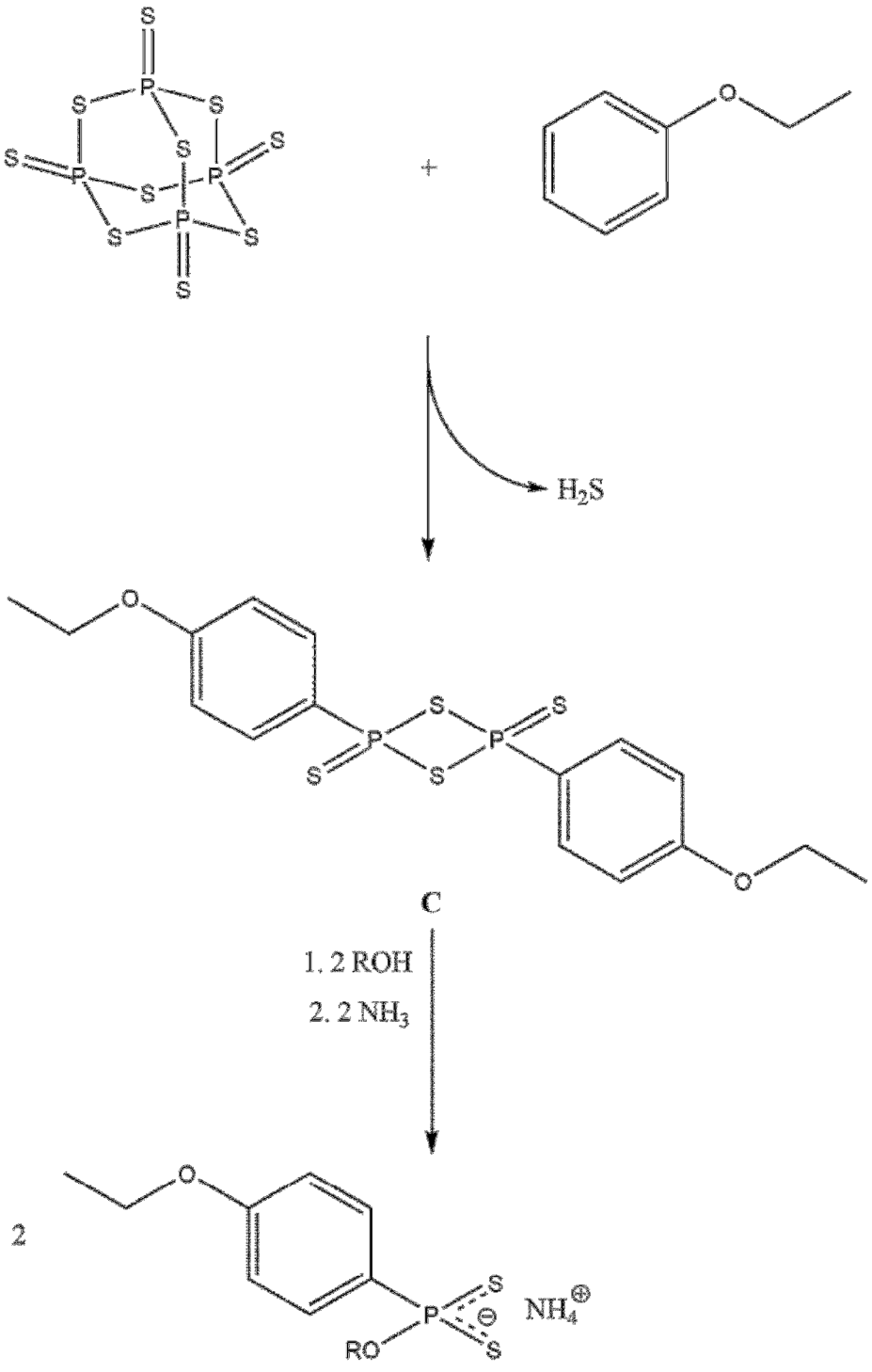

Scheme 1.2: Synthetic route from P_4S_{10} to an ammonium dithiophosphonate salt

The commercial applications of dithiophosphonates exploit the ability of the ligand to form stable metal chelates. Applications include use as anti wear additives in lubricant oils,[18-22]

flotation reagents for the recovery of metals from their solutions in the mining industry,[23] and agricultural pesticides and in chemical warfare.[24] Investigations have been made into the use of dithiophosphonates in the preparation of thin layers by chemical vapour deposition (CVD) or of polymer–inorganic nanocomposites, whereby transition-metal complexes are formed in preliminary steps.[25] Studies have also been conducted into the potential biological and medicinal uses of the transition metal complexes of these compounds, and their adducts.[26, 27]

1.2.1 Resonance and co-ordination modes

Dithiophosphonate ligands have been documented to adopt a variety of co-ordination patterns upon complexation with metal atoms. These variances stem from the resonance structures which the S_2P moiety may adopt, shown in **Figure 1.3**.[15]

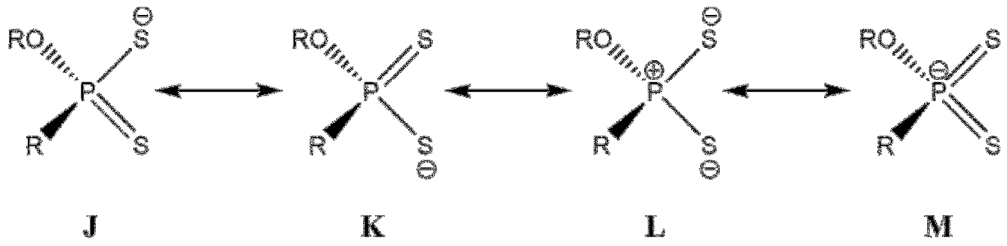

Figure 1.3: Resonance structures of the dithiophosphonate anion

The ligand may engage in either monodentate binding, in cases where the negative charge resides at either sulfur atom, or bidentate binding, when delocalization of this charge occurs across the S-P-S moiety. Thus resonance allows for the formation of mononuclear or multinuclear complexes with the ligand adopting a variety of binding modes dependant on the nature of the metal nucleus to which it is bonded. Common binding modes associated with this class of ligand are shown in **Figure 1.4**.

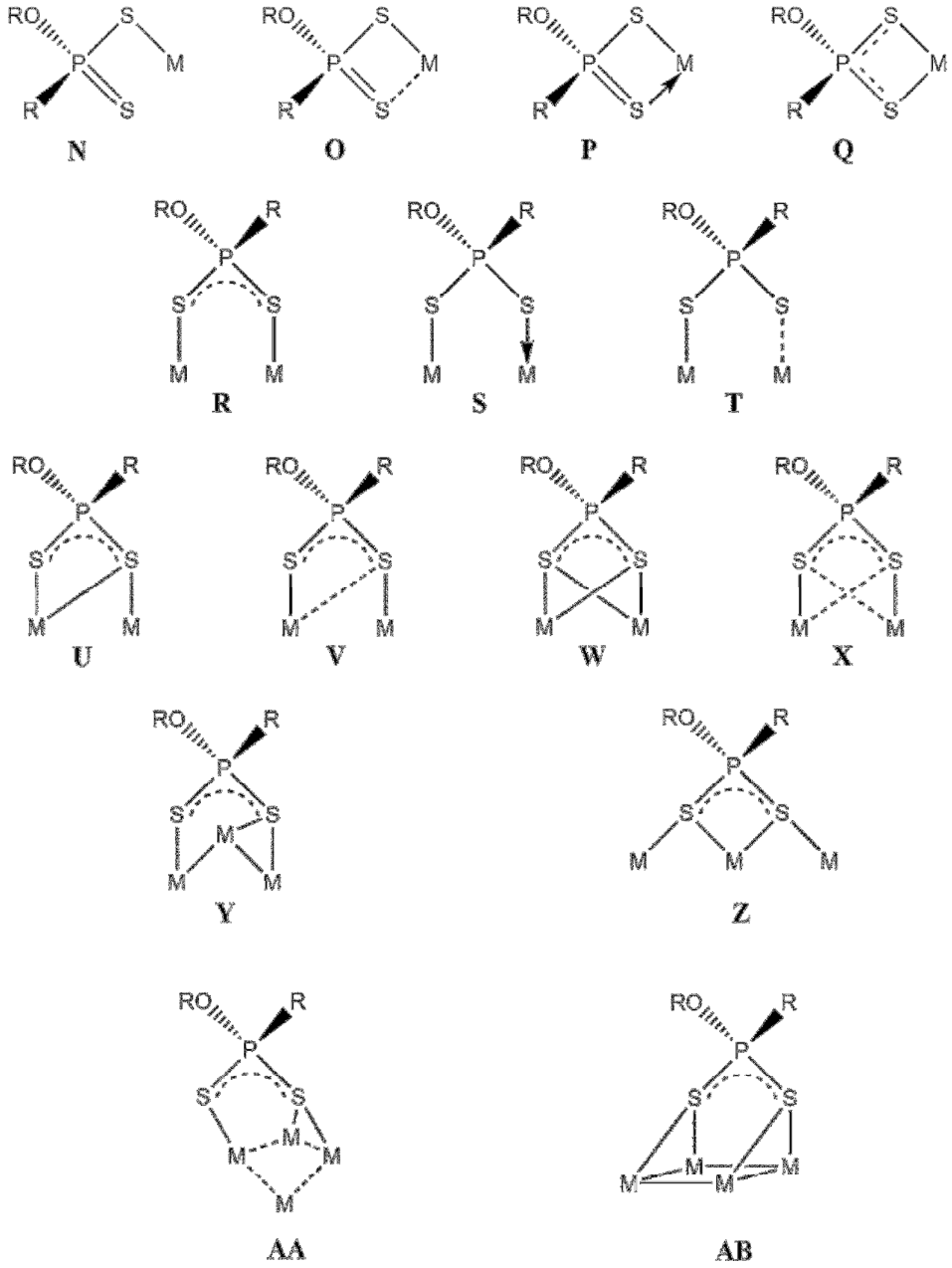

Figure 1.4: Various binding modes associated with metal dithiophosphonate complexes[15]

The Hard and Soft acid-base (HSAB) theory is key to understanding which ligand resonance and thus binding geometry prevails in the varying metal complexes. The theory refers to Lewis acids and bases. In general species termed "Hard" are small (in terms of atomic radius), have high charge states (mainly applied to positive species those termed acids) and

are not easily polarized.[28] For species termed "Soft" the opposite is true, *i.e*. the species have large atomic radii, generally low charge states and are easily polarized. In general 'hard' acids react preferentially, although not exclusively, with hard bases, soft species share a similar affinity for one another.[28] While clear extremes with regards to hardness and softness exist, reagents are deemed either hard or soft respective to the system in which they are placed and the relative hardness or softness of other species within the same system. The dithiophosphonate ligand class are Lewis bases and are generally described as soft species. However, they offer a degree of flexibility as they behave in either a softer or harder fashion, depending on the Lewis acid (the metal ion) to which they are bound. The following description of co-ordination patterns refers to the mononuclear monoconnective and biconnective systems, dinuclear biconnective systems may feature symmetrical or assymetrical interactions of donor S atoms with metal nuclei. Dinuclear triconnective and tetraconnective, trinuclear triconnective and tetraconnective as well as tetranuclear tetraconnective systems have all been observed for P/S type ligands.[15] The general trend previously observed is that soft mononuclear complexes, such as Hg(II) or Au(I), prefer binding to the ligand in a monodentate manner, which is associated with the predominance of resonance structures **J** and **K**. The purely monodentate system features the non-bonding (dangling) S atom retaining a more double bond character to the P atom. However, the observation of either dative (**O**) or anisobidentate (**P**) co-ordinations of the other S atom to the metal centre are not uncommon. Harder metals have been shown to prefer resonance structure **L,** the hard base form of dithiophosphonates. Ni(II) is termed as an intermediary Lewis acid, as it has been shown previously to behave as either 'hard' or 'soft', in reported dithiophosphonate complexes. However, it has shown an affinity for resonance structure **L** thus Ni(II) may be described as behaving as a hard acid in this complex system. In Ni(II) complexes the ligand is bound in a bidentate manner and the bonds are of a more ionic

nature. The exhibited versatility in dithiophosphonate binding modes has motivated studies into these ligands being applied in supramolecular chemistry.

1.2.2 Complexes relevant to this study

Dithiophosphonate complexes of Cd(II), Ni(II), Hg(II), Pb(II) have been previously reported by Woollins and co-workers, the dithiophosphonate ligands reported were derived from methanol, ethanol, 2-propanol and their respective reactions with LR.[17,29] The reaction steps involved in these complexation reactions are relatively simple: stoichiometric equivalents of both ligand and metal are dissolved separately, the metal solution is added to that of the ligand, the formation of a precipitate is indicative of successful complexation, the solid product is isolated by filtration, heating of the reaction was conducted when deemed necessary. In the previously described study by Woollins and co-workers, stoichiometric amounts of metal salts and ligand salts were dissolved in the parent alcohol of the respective ligand to be complexed, and heated to elevated temperatures for the duration of the reaction.

1.2.2.1 Group 10: Nickel

While representative dithiophosphonate complexes of other group 10 metals Pd(II) and Pt(II) have been previously studied,[29, 30] Ni(II) complexes are by far the most widely reported.[17, 31-34] The first nickel(II) dithiophosphonate complex and crystal structure thereof was reported in 1967 by Hartung.[31] The complex synthesized was $[Ni\{S_2PPh(OEt)\}_2]$, it is mononuclear and neutral in nature, which is typical of Ni(II) complexes of this class. The Ni atom generally adopts a square planar geometry in such complexes, favouring resonance mode **L** of the ligand, thus binding in an isobidentate manner, evidenced by equal P-S bond lengths in the solid state.[33, 35] Although isobidentate binding is prevalent, many examples of anisobidentate binding are also noted in literature.[36]

In most cases the nickel atom lies on a centre of inversion about which similar groups of the ligand are observed *trans* to one another, above and below the metal co-ordination plane. An example of this is shown in **Figure 1.5** in which the anisyl groups are shown clearly oriented *trans* to one another.

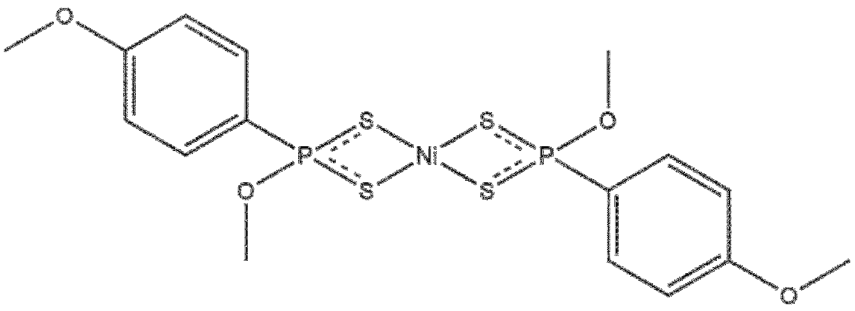

Figure 1.5: A schematic representation of a previously reported *trans* square planar nickel(II)dithiophosphonate complex [17]

The *cis* configuration of such nickel complexes is far rarer in literature, with the first such complex only being reported in 2002 by Verani and co-workers.[37] The synthesis of this complex entailed hydrolysis of the P–N bond in aminated LR, followed by complexation with a Ni(II) salt. The stabilisation of this complex in the solid state was achieved by the formation of an extensive and intricate network of hydrogen bonds. Woollins and co-workers also successfully synthesized a *cis* Ni(II) dithiophosphonate complex in 2003.[36] A *trans* complex of a FcLR based ligand was interconverted to its *cis* isomer by interaction with a secondary ligand, namely pyridine, **Scheme 1.3**. The formation of the *cis* isomer as well as the octahedral intermediate was confirmed by single crystal X-ray diffraction.

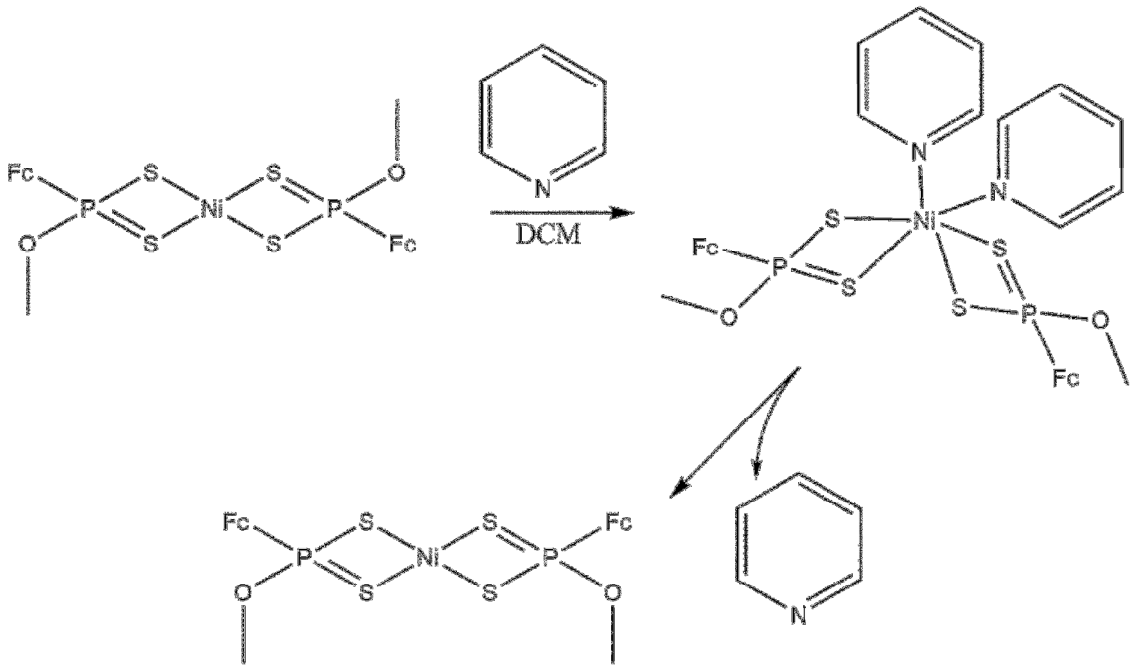

Scheme 1.3: Interconversion of a *trans* Ni(II) dithiophosphonato complex to the *cis* isomer via an intermediary adduct complex

The square planar geometry of nickel complexes in this ligand class allows the metal centre to host secondary ligands,[34, 38-40] thereby achieving a six co-ordinate octahedral system, early examples of these adducts were reported by Porta and co-workers.[40] Reactions of secondary ligands with dithiophosphonate complexes have been investigated by Aragoni and co-workers and have revealed how the increased occupancy of the Ni co-ordination sphere may influence the co-ordination of the dithiophosphonate ligand.[34, 39] It was shown that reaction of the complex $[Ni\{S_2P(4\text{-}C_6H_4OMe)(OMe)\}_2]$ with the secondary ligand 2,4,6-tris(2-pyridyl)-1,3,5-triazine (tptz), yielded an octahedral complex in which the tptz occupied three co-ordination sites, forcing one of the two dithiophosphonate ligands into a monodentate mode while the other remains isobidentate, **Figure 1.6**.[39]

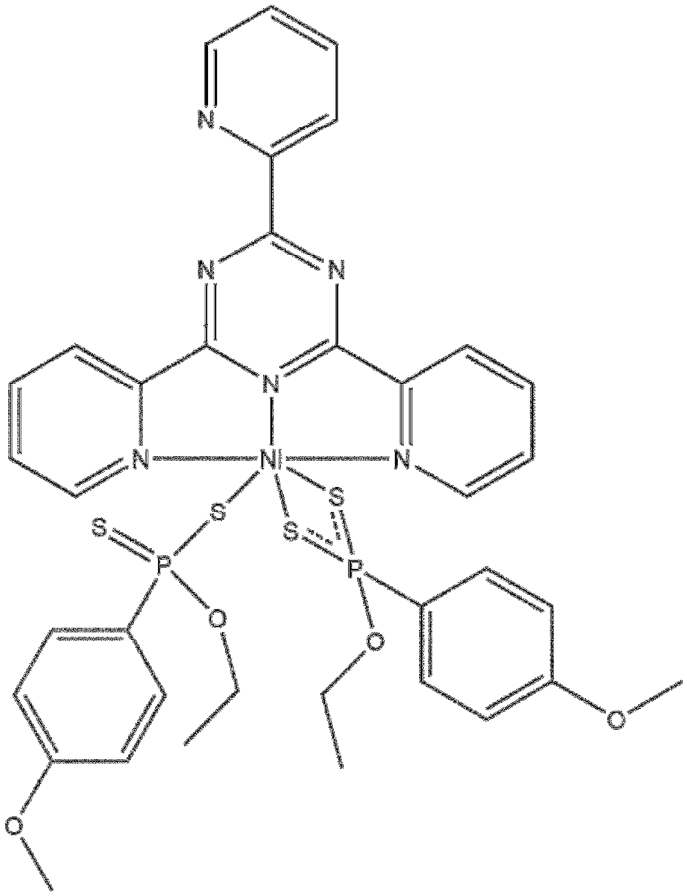

Figure 1.6: Schematic representation of an octahedral nickel(II) dithiophosphonate complex featuring a secondary ligand.[39]

1.2.2.2 Group 12: Cadmium and Mercury

Cadmium, mercury and zinc are group 12 transition metals. Dithiophosphonate complexes of such metals, derived from aliphatic alcohols and LR and phenetole Lawesson's reagent, have been reported and all show a similar co-ordination pattern.[41-44] These metals generally adopt a four co-ordinate pattern and generally favour resonance modes **J** and **K** of the ligand. This is due to Cd(II) and Hg(II) both being soft Lewis acids, while Zn(II) is an intermediate Lewis acid. Five co-ordinate binding of Cd(II) has also been reported.[45] This results in anisobidentate binding of the ligands to the metal nuclei. The complexes are typically

characterized by being dinuclear, *i.e.* two metal atoms are present binding to four ligand anions, two of which bind solely to one metal nucleus each, in a chelating fashion, while the other two bridge the metal nuclei in a biconnective fashion. This results in the formation of an eight-membered ring comprising of two metal atoms, two phosphorus atoms and four sulfur atoms.

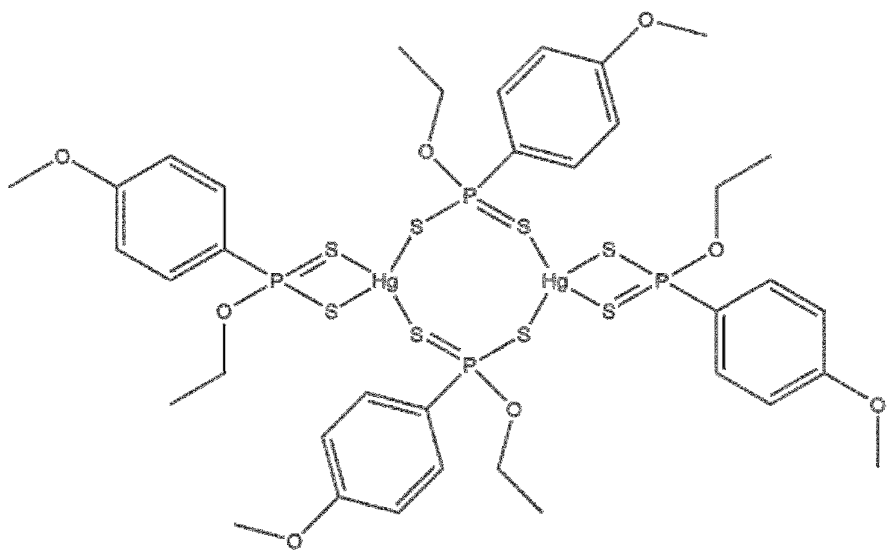

Figure 1.7: An example of a mercury(II) dithiophosphonate type complex[17]

1.2.2.3 Group 14: Lead

Lead(II), like the group 12 metals, is known to favour resonance structures **J** and **K** of the dithiophosphonate ligand, as it too is a soft acid**,** thus ligand binding is generally anisobidentate. The ligand is generally diconnective with both mononuclear and dinuclear systems previously observed.[17,36,46] The earliest Pb(II) crystallographically studied complex is bis[(isopropoxy)ferrocenyldithiophonato]lead(II) reported by Woollins *et al.*. This structure was reported as an infinite polymeric chain composed of monomeric units in which the lead nuclei sit at the apexes of distorted pyramids each having a basal plain consisting of four

sulfur atoms, the monomers were linked by Pb···S interactions of neighbouring units (**Figure 1.8 i**).[36] A second crystallographic motif, similar to the earlier reported structure, has been observed, again the structures featured monomeric units of the type $Pb(S_2PR'OR)_2$, where R' = Ferrocenyl or anisyl groups and R = 2-propyl, however instead of infinite polymeric chains, dimeric pairs of two monomer units were reported (**Figure 1.8 ii**).[17,46]

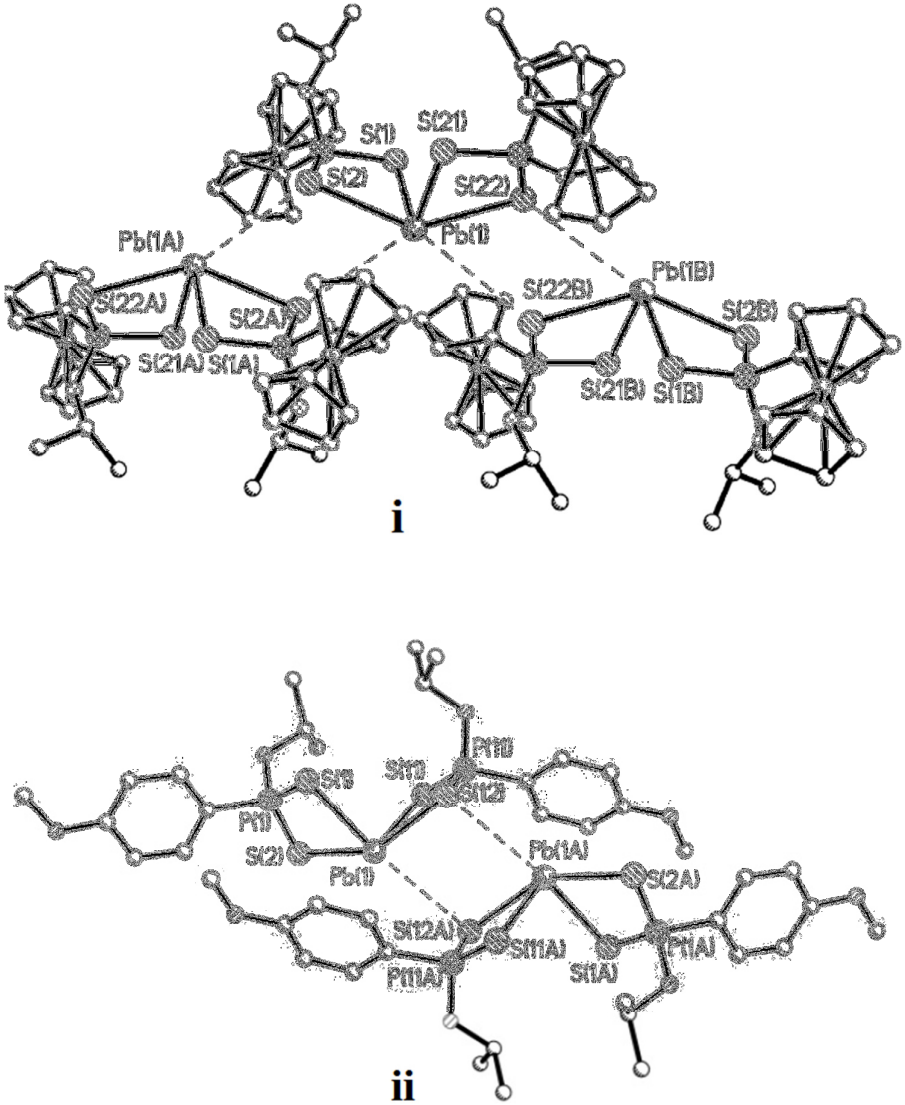

Figure 1.8: Crystal structures of distorted pyramidal lead(II) dithiophosphonate complexes featuring intermolecular Pb···S interactions [17]

Woollins *et al.* also reported the formation of a third type of lead dithiophosphonate crystal structure, which is also polymeric in nature.[17] However, instead of featuring Pb···S interactions between monomeric units, covalent bonding was shown to be the sole force holding the polymer together. Each lead atom was shown to bind to four sulfur atoms, each originating from four separate dithiophosphonate ligands. The ligands were thereby shown to bridge Pb atoms thus creating the polymer chain.[17]

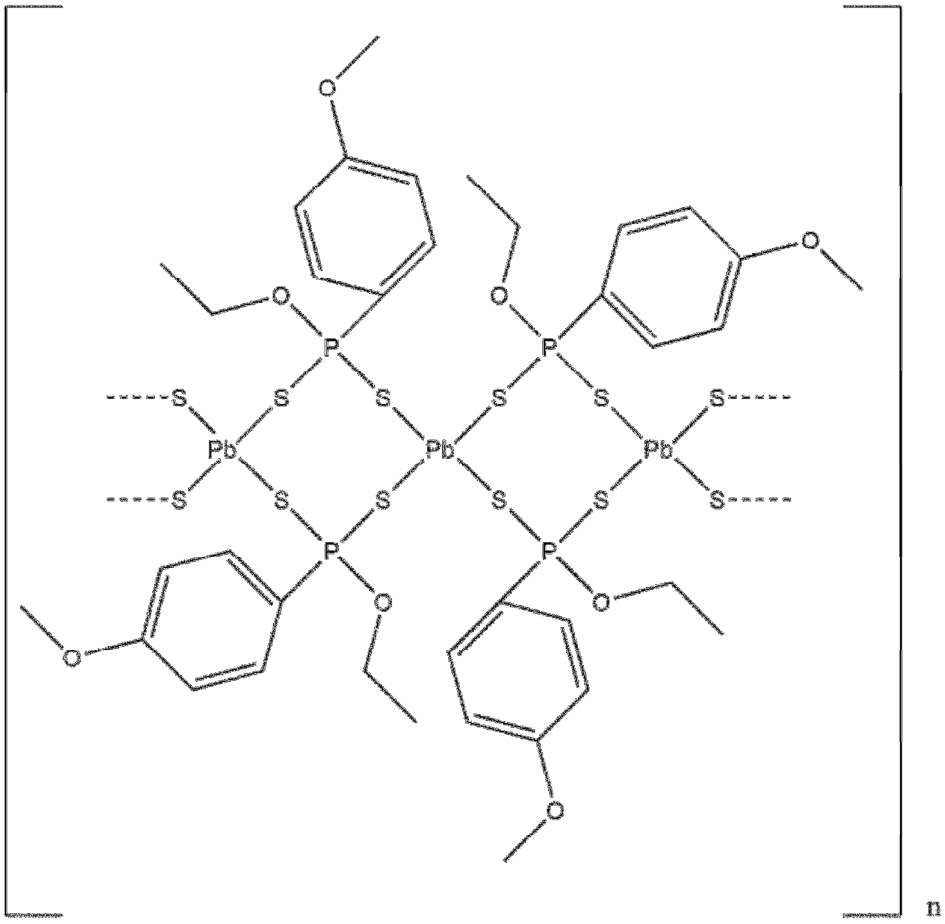

Figure 1.9: A covalently linked polymeric lead(II)dithiophosphonate complex[17]

1.3 Aims and Objectives of the study

The main objectives of the study undertaken are:

- Synthesis and characterization of new dithiophosphonate ligand systems based on phenetole Lawesson's reagent and various aliphatic alcohols.
- Synthesis and characterization of new metal complexes.
- Fully characterize all new compounds isolated using NMR spectroscopy (^{31}P, ^{13}C, ^{1}H), IR spectroscopy and elemental analysis.
- Conduct X-ray crystallographic studies of new complexes.
- Draw comparison and highlight differences (if any) in results obtained to previously reported data of related complexes.
- Thus the overall objective was to determine if small changes in starting materials could lead to significant changes in structure of metal dithiophosphonato complexes.

1.4 Overview

This dissertation has been divided into 5 distinct chapters.

Chapter 1: The present chapter serves as a comprehensive introduction into the dithiophosphonate ligand class including the role of diphosphetane disulfide dimers as important starting materials in ligand synthesis, the phosphor-1,1-dithiolato compounds (the group to which the subject ligand subclass belongs), the main synthetic routes to dithiophosphonates, the resonance influenced co-ordination patterns of this subclass and metal complexes similar to those investigated in this study.

Chapter 2: This chapter contains comprehensive experimental data pertaining to the preparation of new compounds synthesised in this study as well as preparation of phenetole Lawesson's reagent, a primary starting material. A summary of characterization data is contained herein including NMR (^{31}P, ^{13}C, ^{1}H) spectroscopic data, selected IR bands, elemental analysis and melting points.

Chapter 3: contains the results and discussion of ligand synthesis and the four new nickel(II) complexes synthesized as well as an octahedral nickel adduct complex. Crystallographic data of the nickel complexes is represented herein.

Chapter 4 contains the results and discussion of two new dinuclear mercury(II) complexes and one new dinuclear cadmium complex. Crystallographic data of the aforementioned complexes is represented herein.

Chapter 5 describes a new dimeric lead(II) complex synthesized including a discussion of crystallographic data.

Chapter 6 serves as the concluding chapter in which the principal findings of the study are highlighted and possible future work proposed.

1.5 References

1. R. Murugavel, A. Choudhury, M. G. Walawalkar, R. Pothiraja and C. N. R. Rao, *Chem. Rev. (Washington, DC, U. S.)*, 2008, **108**, 3549-3655.
2. W. E. Van Zyl, *Comments Inorg. Chem.*, 2010, **31**, 13-45.
3. W. E. Van Zyl and J. P. Fackler, *Phosphorus, Sulfur Silicon Relat. Elem.*, 2000, **167**, 117-132.
4. I. Haiduc, G. Mezei, R. Micu-Semeniuc, F. T. Edelmann and A. Fischer, *Z. Anorg. Allg. Chem.*, 2006, **632**, 295-300.
5. P. Fay and H. P. Lankelma, *J. Am. Chem. Soc.*, 1952, **74**, 4933-4935.
6. P. E. Newallis, J. P. Chupp and L. C. D. Groenweghe, *J. Org. Chem.*, 1962, **27**, 3829-3831.
7. M. R. S. J. Foreman, A. M. Z. Slawin and J. D. Woollins, *Dalton Trans.*, 1996, 3653-3657.
8. J. D. Woollins, *Synlett*, 2012, **2012**, 1154-1169.
9. M. J. Pilkington, A. M. Z. Slawin, D. J. Williams, P. T. Wood and J. D. Woollins, *Heteroat. Chem.*, 1990, **1**, 351-355.
10. I. P. Gray, P. Bhattacharyya, A. M. Z. Slawin and J. D. Woollins, *Chem.--Eur. J.*, 2005, **11**, 6221-6227.
11. G. Hua, Y. Li, A. M. Z. Slawin and J. Derek Woollins, *Tetrahedron*, 2008, **64**, 5442-5448.
12. I. P. Gray, A. M. Z. Slawin and J. D. Woollins, *Dalton Trans.*, 2005, 2188-2194.
13. P. Bhattacharyya, A. M. Z. Slawin and J. D. Woollins, *Angew. Chem., Int. Ed.*, 2000, **39**, 1973-1975.
14. Z. Kaleta, B. T. Makowski, T. Soós and R. Dembinski, *Org. Lett.*, 2006, **8**, 1625-1628.

15. I. Haiduc, D. B. Sowerby and S.-F. Lu, *Polyhedron*, 1995, **14**, 3389-3472.

16. I. Haiduc and D. B. Sowerby, *Polyhedron*, 1996, **15**, 2469-2521.

17. I. P. Gray, A. M. Z. Slawin and J. D. Woollins, *Dalton Trans.*, 2004, 2477-2486.

18. S. L. Lawton and G. T. Kokotailo, *Inorg. Chem.*, 1969, **8**, 2410-2421.

19. S. L. Lawton, W. J. Rohrbaugh and G. T. Kokotailo, *Inorg. Chem.*, 1972, **11**, 612-618.

20. P. G. Harrison, M. J. Begley, T. Kikabhai and F. Killer, *Dalton Trans.*, 1986, 925-928.

21. D.Klaman, Lubricants and related products,*Verlag-Chemie, Weinheim*, 1984.

22. A. M. Barnes, K. D. Bartle and V. R. A. Thibon, *Tribol. Int.*, 2001, **34**, 389-395.

23. I. P. Alimarin, V. R. Tat'yana and M. I. Vadim, *Russ. Chem. Rev.*, 1989, **58**, 863.

24. R. S. Edmundson, *Dictionary of organophosphorus compounds*, Chapman and Hall, London , 1988.

25. M. Gianini, W. R. Caseri, V. Gramlich and U. W. Suter, *Inorg. Chim. Acta*, 2000, **299**, 199-208.

26. J. S. Casas, A. Castiñeiras, M. A. C. Rodríguez-Argüelles, A. N. Sánchez, J. Sordo, A. Vázquez López, S. Pinelli, P. Lunghi, P. Ciancianaini, A. Bonati, P. Dall'Aglio and R. Albertini, *J. Inorg. Biochem.*, 1999, **76**, 277-284.

27. W. J. Stec, B. Uznanski, A. Wilk, B. L. Hirschbein, K. L. Fearon and B. J. Bergot, *Tetrahedron Lett.*, 1993, **34**, 5317-5320.

28. R. G. Pearson, *J. Am. Chem. Soc.*, 1963, **85**, 3533-3539.

29. M. C. Aragoni, M. Arca, F. Demartin, Francesco A. Devillanova, C. Graiff, F. Isaia, V. Lippolis, A. Tiripicchio and G. Verani, *Eur. J. Inorg. Chem.*, 2000, **2000**, 2239-2244.

30. J. P. Fackler Jr and L. D. Thompson Jr, *Inorg. Chim. Acta*, 1981, **48**, 45-52.

31. H. Hartung, *Z. Chem.*, 1967, **7**, 241-241.

32. Y. Ozcan, S. Ide, M. Karaku and H. Yilmaz, *Anal. Sci.*, 2002, **18**, 1285-1286.

33. M. Arca, A. Cornia, F. A. Devillanova, A. C. Fabretti, F. Isaia, V. Lippolis and G. Verani, *Inorg. Chim. Acta*, 1997, **262**, 81-84.

34. M. C. Aragoni, M. Arca, F. A. Devillanova, M. B. Hursthouse, S. L. Huth, F. Isaia, V. Lippolis, A. Mancini, S. Soddu and G. Verani, *Dalton Trans.*, 2007, 2127-2134.

35. A. Gataulina, D. Safin, T. Gimadiev and M. Pinus, *Transition Met. Chem. (London)*, 2008, **33**, 921-924.

36. I. P. Gray, H. L. Milton, A. M. Z. Slawin and J. D. Woollins, *Dalton Trans.*, 2003, 3450-3457.

37. V. G. Albano, M. C. Aragoni, M. Arca, C. Castellari, F. Demartin, F. A. Devillanova, F. Isaia, V. Lippolis, L. Loddo and G. Verani, *Chem. Commun.*, 2002, 1170-1171.

38. M. C. Aragoni, M. Arca, M. Crespo, F. A. Devillanova, M. B. Hursthouse, S. L. Huth, F. Isaia, V. Lippolis and G. Verani, *CrystEngComm*, 2007, **9**, 873-878.

39. M. C. Aragoni, M. Arca, M. Crespo, F. A. Devillanova, M. B. Hursthouse, S. L. Huth, F. Isaia, V. Lippolis and G. Verani, *Dalton Trans.*, 2009, 2510-2520.

40. P. Porta, A. Sgamellotti and N. Vinciguerra, *Inorg. Chem.*, 1971, **10**, 541-547.

41. S. Blaurock, F. T. Edelmann, I. Haiduc, G. Mezei and P. Poremba, *Inorg. Chim. Acta*, 2008, **361**, 407-410.

42. M. Karakus, H. Yilmaz and E. Bulak, *Russ. J. Coord. Chem.*, 2005, **31**, 316-321.

43. M. Karakus, H. Yilmaz, E. Bulak and P. Lönnecke, *Appl. Organomet. Chem.*, 2005, **19**, 396-397.

44. M. Karakus and H. Yilmaz, *Russ. J. Coord. Chem.*, 2006, **32**, 437-443.

45. W. Shi, M. Shafaei-Fallah, C. E. Anson and A. Rothenberger, *Dalton Trans.*, 2006, 3257-3262.

46. I. P. Gray, A. M. Z. Slawin and J. D. Woollins, *Z. Anorg. Allg. Chem.*, 2004, **630**, 1851-1857.

Chapter 2: Experimental

2.1 General considerations

All ligand preparations were conducted under inert, dry N_2 atmosphere using standard Schlenk techniques and dry solvents. Complexation and oxidation reactions were conducted in an open atmosphere. All glassware was cleaned and dried at 140 °C for 24 hours prior to use. Stirring was achieved using a magnetic stirrer bar and all heating was conducted by means of immersion in a silicone oil bath. Room temperature refers to 296-298 K. Solvents used were distilled prior to drying under N_2. Dichloromethane and toluene were dried over anhydrous calcium chloride. Diethyl ether and hexane were dried over sodium wire using benzophenone as an indicator of dryness. Solvents were degassed prior to their immediate use. Deuterated solvents methanol-d4 and $CDCl_3$ were supplied by Merck. The alcohols used were methanol, 2-propanol, 1-propanol, 2-butanol and 1-butanol, and were supplied by Sigma Aldrich. All alcohols were distilled over magnesium turnings/iodine prior to use. Cadmium nitrate tetrahydrate was supplied by Riedel de Haen, mercury chloride monohydrate was supplied by Merck, and lead nitrate was supplied by Associated Chemical Entreprises. Iodine, magnesium turnings and nickel chloride hexahydrate were supplied by SAARCHEM. All metal salts were used as supplied. Nitrogen and ammonia were supplied by Afrox. Any water used in synthesis refers to deionised water. Benzophenone, phosphorus pentasulfide (P_4S_{10}) and phenetole 99% were supplied by Sigma Aldrich.

2.2 Instrumentation

Proton ^{1}H (400 MHz), ^{13}C (100 MHz) and ^{31}P (162 MHz) NMR spectra were obtained using a Bruker Avance III 400 MHz NMR spectrometer under ambient conditions. Phosphorus ^{31}P nuclei chemical shifts were referenced externally relative to a triphenylphosphine shift of -17.6 ppm. Proton ^{1}H nucleus chemical shifts were referenced relative to residual proton impurities in the deuterated solvents at 7.24 ppm for $CDCl_3$ and 4.78 ppm for methanol-d4, ^{13}C shifts were referenced similarly to solvent shifts of 77.23 ppm for $CDCl_3$ and 49.2 ppm for methanol-d4. Infrared spectra were collected on a Perkin Elmer Spectrum 100 FTIR spectrophotometer. Elemental analyses were performed at the University of Kwazulu-Natal Pietermaritzburg campus using a Thermo Scientific Flash 2000 elemental analyzer.

Single crystal X-ray diffraction studies on compounds **2A** , **2B** and **2D** were performed at the University of Cape Town using a Nonius Kappa-CCD diffractometer using graphite monochromated MoKα radiation (λ = 0.71073 Å). Temperature was controlled by an Oxford Cryostream cooling system (Oxford Cryostat). The data collections was evaluated using the Bruker Nonius "Collect" program.[1] Data was scaled and reduced using DENZO-SMN software.[2] Absorption correction was performed using SADABS.[3]

Crystallographic data collection and refinement of compounds **1A**, **3A**, **4A**, **4Ai**, **1B** and **1C** was conducted at the University of Kwazulu-Natal Westville Campus, using a Bruker Kappa DUO APEX II diffractometer, also using graphite monochromated MoKα radiation (λ = 0.71073 Å) with refinements and data reduction being made using SAINT software.[4]

The structural data collected at both centres were solved by direct methods and refined employing full-matrix least-squares with the program SHELXL-97[5] refining on F^2. All hydrogen atoms were found in the difference electron density maps and were placed in idealised positions and refined with geometrical constraints. The parameters for crystal data

collection and structure refinements, the bond lengths, angles, torsion angles are contained in respective *cif* files in the appendix on the accompanying compact disc.

Crystallographic images in this thesis were prepared using ORTEP-3[6] and Mercury[7] software.

2.3 Safety considerations

All organophosphorus compounds synthesised in this study evolve H_2S upon exposure to atmosphere and caution must be taken when handling them. All the procedures described hereafter were conducted in a well-ventilated fume hood with great caution being exercised to minimize exposure to fumes of any kind.

2.4 Starting materials

2.4.1 Preparation of 2,4-bis(4-ethoxyphenyl)-1,3,2,4-dithiadiphosphetane-2,4-disulfide (phenetole Lawesson's Reagent)[8]

Phosphorus pentasulfide (15.194 g , 0.03418 mol) was placed in a 500 mL two necked round bottomed flask equipped with a nitrogen inlet. Phenetole (30 g , 0.2456 mol) was added to the flask. The mixture was stirred and heated to reflux until all solids had dissolved over a period of 6 hours. The resulting clear yellow solution was allowed to cool down slowly to room temperature, resulting in the formation of a white crystalline material. This material was isolated by vacuum filtration and washed with toluene, followed by washing with portions of diethyl ether. The resulting highly insoluble white powder was stored in a vacuum desiccator. Melting point 214 -215 °C decomposed. Product insoluble in $CDCl_3$ and methanol-D4.

2.5 Ligands

2.5.1 Synthesis of $(NH_4)[S_2P(4\text{-}C_6H_4OEt)(OCH_3)]$ (1)

A Schlenk flask was charged with $(4\text{-}C_6H_4OEtP(S)S)_2$ (5.346 g, 0.01236 mol) and held under a vacuum for 15 minutes. Thereafter the flask was flushed with N_2 and methanol (0.8 g, 0.02497 mol) was added. The mixture was heated to 70 °C until no visible white solids were visible after about 90 minutes, and the reaction mixture was agitated periodically by shaking the reaction vessel. The resulting viscous, clear, colourless liquid was cooled to room temperature, and cooled down further in an ice bath. While still in the ice bath, ammonia gas was bubbled through the liquid *via* a glass needle. Heat was evolved and the clear liquid formed a white solid. Diethyl ether was added to the vessel, which was then stirred for a period of 30 minutes, whilst more ammonia was bubbled through the resulting suspension. The diethyl ether was removed *in vacuo* and the resulting fine white powder was stored in a vacuum desiccator. Yield 4.859 g (74%). Melting point 161 - 162 °C.

^{31}P NMR (methanol-D4): δ (ppm): 109.37. ^{1}H NMR (methanol-D4): δ (ppm): 7.94 (2H, dd, $J(^{31}P\text{-}^{1}H)$ = 13.44 Hz, $J(^{1}H\text{-}^{1}H)$ =8.8 Hz, *ortho*-ArH) , 6.81 (2H, dd, $J(^{31}P\text{-}^{1}H)$ = 8.86 Hz, $J(^{1}H\text{-}^{1}H)$ =2.62 Hz, *meta*-ArH), 4.00 (2H, quart, $J(^{1}H\text{-}^{1}H)$ = 6.99 Hz, $ArOCH_2$), 3.47 (3H, d, $J(^{31}P\text{-}^{1}H)$=14.64 Hz, CH_3), 1.32 (3H, t, $J(^{1}H\text{-}^{1}H)$ = 6.98 Hz, $ArOCH_2CH_3$). ^{13}C NMR (Methanol-D4): δ (ppm): 161.96 (*para*-ArC), 135.65 (*ipso*-ArC), 133.05 (*meta*-ArC), 114.38 (*ortho*-ArC), 64.67 ($ArOCH_2$), 51.22 (CH_3), 15.28 ($ArOCH_2CH_3$).

Selected IR data ν/cm^{-1}: 3087-2934 (b), 1176 (m), 1042 (m), 667 (s), 556 (s)

Similar preparation methods and techniques to those used for compound **1** were used to prepare compounds **2**, **3** and **4**. Thus only variances from the above method are noted in each of the respective preparation sections for compounds **2**-**4** below.

2.5.2 Synthesis of $(NH_4)[S_2P(4\text{-}C_6H_4OEt)(OCH(CH_3)_2)]$ (2)

Mass of $(4\text{-}C_6H_4OEtP(S)S)_2$ used: 4.494 g, 0.01039 mol. Alcohol used: 2-propanol. Alcohol mass: 1.252 g, 0.02083 mol. Reaction temperature: 70 °C. Reaction time: 120 min. Product appearance: fine white powder. Yield 5.225 g (85%). Melting point 184 - 185 °C.

^{31}P NMR (Methanol-D4): δ (ppm): 104.32. ^{1}H NMR (Methanol-D4): δ (ppm): 7.96 (2H, dd, $J(^{31}P\text{-}^{1}H)$ = 13.4 Hz, $J(^{1}H\text{-}^{1}H)$ = 8.68 Hz, *ortho*-ArH) , 6.80 (2H, dd, $J(^{31}P\text{-}^{1}H)$ = 8.8 Hz, $J(^{1}H\text{-}^{1}H)$ = 2.60 Hz, *meta*-ArH), 4.62 (1H, d quart, $J(^{31}P\text{-}^{1}H)$ = 20.9 Hz, $J(^{1}H\text{-}^{1}H)$ = 6.19 Hz, CH), 4.00 (2H, quart, $J(^{1}H\text{-}^{1}H)$ = 7.00 Hz, $ArOCH_2$), 1.32 (3H, t, $J(^{1}H\text{-}^{1}H)$ = 7 Hz, $ArOCH_2CH_3$), 1.13 (6H, d, $J(^{1}H\text{-}^{1}H)$ = 6.16 Hz, CH_3). ^{13}C NMR (Methanol-D4): δ (ppm): 161.85 (*para*-ArC), 136.98 (*ipso*-ArC), 133.09 (*meta*-ArC), 114.30 (*ortho*-ArC), 69.98 (CH), 64.67($ArOCH_2$), 25.45 (CH_3), 15.30 ($ArOCH_2CH_3$).

Selected IR data ν/cm^{-1}: 3175-2812 (b), 1179 (m), 1040 (m), 666 (s), 565 (s)

2.5.3 Synthesis of $(NH_4)[S_2P(4\text{-}C_6H_4OEt)(OCH_2CH_2CH_3)]$ (3)

Mass of $(4\text{-}C_6H_4OEtP(S)S)_2$ used: 8.012 g, 0.01850 mol. Alcohol used: 1-propanol. Alcohol mass: 2.228 g, 0.03708 mol. Reaction temperature: 80 °C. Reaction time: 180 min. Stirring in diethyl ether was carried out overnight. Product appearance: fine white powder. Yield 9.547 g (88%). Melting point 148 - 150 °C.

^{31}P NMR (Methanol-D4): δ (ppm): 106.60. ^{1}H NMR (Methanol-D4): δ (ppm): 7.92 (2H, dd, $J(^{31}P\text{-}^{1}H)$ = 13.36 Hz, $J(^{1}H\text{-}^{1}H)$ = 8. 68 Hz, *ortho*-ArH) , 6.79 (2H, dd, $J(^{31}P\text{-}^{1}H)$ = 8.82 Hz, $J(^{1}H\text{-}^{1}H)$ = 3.06 Hz, *meta*-ArH), 4.26 (2H, d trip, $J(^{31}P\text{-}^{1}H)$ = 20.9 Hz, $J(^{1}H\text{-}^{1}H)$ = 7.89 Hz, CH_2), 4.00 (2H, quart, $J(^{1}H\text{-}^{1}H)$ = 7.00 Hz, $ArOCH_2$), 1.32 (3H, t, $J(^{1}H\text{-}^{1}H)$ = 7 Hz, $ArOCH_2CH_3$), 1.13 (6H, d, $J(^{1}H\text{-}^{1}H)$ = 6.16 Hz, CH_3). ^{13}C NMR (Methanol-D4): δ (ppm): 161.85 (*para*-ArC), 136.98 (*ipso*-ArC), 133.09 (*meta*-ArC), 114.30 (*ortho*-ArC), 69.98 (CH), 64.67($ArOCH_2$), 25.45 (CH_3), 15.30 ($ArOCH_2CH_3$).

Selected IR data ν/cm^{-1}: 3140-2832 (b), 1178 (m), 1041 (m), 674 (s), 562 (s)

2.5.4 Synthesis of $(NH_4)[S_2P(4\text{-}C_6H_4OEt)(OCH(CH_3)_2CH_3)]$ (4)

Mass of $(4\text{-}C_6H_4OEtP(S)S)_2$ used: 5.210 g, 0.01205 mol. Alcohol used: 2-butanol. Alcohol mass: 1.786 g, 0.02409 mol. Reaction temperature: 80 °C. Reaction time: 120 min. Product appearance: fine white powder. Yield 6.333 g (85%). Melting point 135 - 136 °C.

^{31}P NMR ($CDCl_3$): δ (ppm): 104.96. ^{1}H NMR ($CDCl_3$): δ (ppm): 7.96 (2H, dd, J(^{31}P-^{1}H) = 13.6 Hz, J(^{1}H -^{1}H) = 8.80 Hz, *ortho*-ArH) , 6.79 (2H, dd, J(^{31}P-^{1}H) = 8.84 Hz, J(^{1}H -^{1}H) = 2.60 Hz, *meta*-ArH), 4.49 (1H, d quart, J(^{31}P-^{1}H) = 26.89 Hz, J(^{1}H -^{1}H) = 6.14 Hz, CH), 3.99 (2H, quart, J(^{1}H -^{1}H) = 6.99 Hz, $ArOCH_2$), 1.49 (2H, m, J(^{1}H -^{1}H) = 7.26 Hz, $OCH(CH_3)\mathbf{CH_2}CH_3$) 1.32 (3H, t, J(^{1}H -^{1}H) = 7.00 Hz, $ArOCH_2CH_3$), 1.12 (3H, d, J(^{1}H -^{1}H) = 6.32 Hz, $OCH(\mathbf{CH_3})CH_2CH_3$), 0.78 (3H, t, J(^{1}H -^{1}H) = 7.50 Hz, $OCH(CH_3)CH_2\mathbf{CH_3}$) . ^{13}C NMR ($CDCl_3$): δ (ppm): 161.71 (*para*-ArC), 138.52 (*ipso*-ArC), 133.11 (*meta*-ArC), 114.16 (*ortho*-ArC), 74.54 (CH), 64.61 ($ArOCH_2$), 31.81 ($OCH(CH_3)\mathbf{CH_2}CH_3$), 21.61 ($OCH(\mathbf{CH_3})CH_2CH_3$), 15.26 ($ArOCH_2CH_3$), 10.13 ($OCH(CH_3)CH_2\mathbf{CH_3}$).

Selected IR data ν/cm^{-1}: 3149-2817 (b), 1178 (m), 1043(m), 667 (s), 556 (s)

2.6 Nickel Complexes

2.6.1 Synthesis of $Ni[S_2P(4\text{-}C_6H_4OEt)(OCH_3)]_2$ (1A)[9]

A beaker was charged with $(NH_4)[S_2P(4\text{-}C_6H_4OEt)(OCH_3)]$ (1.044 g, 4.474 mmol) dissolved in methanol (40 mL) forming a clear colourless solution. A second solution containing nickel chloride hexahydrate ($NiCl_2{\cdot}6H_2O$, 0.540 g, 2.272 mmol) in deionised water (20 mL) was

prepared giving a clear green solution. The nickel solution was added to the dithiophosphonato ligand while stirring over a period of 5 minutes. This resulted in the formation of copious amounts of purple precipitate indicating the formation of the desired complex. The precipitate was collected by vacuum filtration, washed with water (3 x 10 mL) and allowed to dry under vacuum for a period of 3 hours, yielding a crystalline purple powder (1.004 g, 41% yield). Purple coloured crystals suitable for X-ray analysis were grown by vapour diffusion of hexane (8 mL) into a dichloromethane solution of $Ni[S_2P(4\text{-}C_6H_4OEt)(OCH_3)]_2$ (0.352 g, 0.636 mmol in 4 mL). Melting point: 168°C. Elemental % composition found (analytical calculation for $C_{18}H_{24}O_4P_2S_4Ni$): C 39.93 (39.07), H 4.19 (4.37).

^{31}P NMR ($CDCl_3$): δ (ppm): 104.56. ^{1}H NMR ($CDCl_3$): δ (ppm): 7.94 (2H, dd, $J(^{31}P\text{-}^{1}H)$ = 12.76 Hz, $J(^{1}H\text{-}^{1}H)$ =10.08 Hz, *ortho*-ArH) , 6.95 (2H, dd, $J(^{31}P\text{-}^{1}H)$ = 8.76 Hz, $J(^{1}H\text{-}^{1}H)$ =3.08 Hz, *meta*-ArH), 4.07 (2H, quart, $J(^{1}H\text{-}^{1}H)$ = 6.96 Hz, $ArOCH_2$), 3.96 (3H, d, $J(^{31}P\text{-}^{1}H)$=14.8 Hz, CH_3), 1.41 (3H, t, $J(^{1}H\text{-}^{1}H)$ = 6.98 Hz, $ArOCH_2CH_3$). ^{13}C NMR ($CDCl_3$): δ (ppm): 162.64 (*para*-ArC), 131.78 (*meta*-ArC), 128.68 (*ipso*-ArC), 114.62 (*ortho*-ArC), 63.99 ($ArOCH_2$), 52.73 (CH_3), 14.85 ($ArOCH_2CH_3$).

Selected IR data ν/cm^{-1}: 1181 (m), 1034(m), 688 (s), 560 (s)

2.6.2 Synthesis of $Ni[S_2P(4\text{-}C_6H_4OEt)(OCH(CH_3)_2)]_2$ (2A)[10]

A beaker was charged with $(NH_4)[S_2P(4\text{-}C_6H_4OEt)(OCH(CH_3)_2)]$ (0.982 g, 3.347 mmol) which was dissolved in methanol (40 mL) forming a clear colourless solution. A second solution containing nickel chloride hexahydrate ($NiCl_2{\cdot}6H_2O$, 0.399 g, 1.679 mmol) in deionised water (20mL) was prepared giving a clear green solution. The nickel solution was added to that of the dithiophosphonato ligand while stirring over a period of 5 minutes, this resulted in the formation of copious amounts of purple precipitate indicating the formation of

the desired complex. The precipitate was collected by vacuum filtration on a Buchner funnel, washed with water (3 x 10 mL) and allowed to dry under vacuum for a period of 3 hours, yielding a crystalline purple coloured powder (0.761 g, 75% yield). Purple crystals suitable for X-ray analysis were grown by vapour diffusion of hexane (8 mL) into a dichloromethane solution of the $Ni[S_2P(4\text{-}C_6H_4OEt)(OCH(CH_3)_2)]_2$ (0.320 g, 0.525 mmol in 4 mL). Melting point: 168-169°C. Elemental % composition found (analytical calculation for $C_{22}H_{32}O_4P_2S_4Ni$) : C 44.03 (43.36), H 5.10 (5.29).

^{31}P NMR ($CDCl_3$): δ (ppm): 97.96. ^{1}H NMR ($CDCl_3$): δ (ppm): 7.96 (2H, dd, $J(^{31}P\text{-}^{1}H)$ = 13.9 Hz, $J(^{1}H\text{-}^{1}H)$ = 8.66 Hz, *ortho*-ArH) , 6.95 (2H, dd, $J(^{31}P\text{-}^{1}H)$ = 8.74 Hz, $J(^{1}H\text{-}^{1}H)$ = 2.90 Hz, *meta*-ArH), 5.19 (1H, d quart, $J(^{31}P\text{-}^{1}H)$ = 20 Hz, $J(^{1}H\text{-}^{1}H)$ = 6.27 Hz, CH), 4.06 (2H, quart, $J(^{1}H\text{-}^{1}H)$ = 6.97 Hz, $ArOCH_2$), 1.42 (3H, t, $J(^{1}H\text{-}^{1}H)$ = 7 Hz, $ArOCH_2CH_3$), 1.38 (6H, d, $J(^{1}H\text{-}^{1}H)$ = 6.32 Hz, CH_3). ^{13}C NMR ($CDCl_3$): δ (ppm): 162.22 (*para*-ArC), 131.71 (*meta*-ArC), 128.04 (*ipso*-ArC), 114.44 (*ortho*-ArC), 72.10 (CH), 63.76($ArOCH_2$), 24.30 (CH_3), 14.67 ($ArOCH_2CH_3$).

Selected IR data ν/cm^{-1}: 1181 (m), 1035(m), 684 (s), 542 (s)

2.6.3 Synthesis of $Ni[S_2P(4\text{-}C_6H_4OEt)(OCH_2CH_2CH_3)]_2$ (3A)[11]

A beaker was charged with $(NH_4)[S_2P(4\text{-}C_6H_4OEt)(OCH_2CH_2CH_3)]$ (0.997 g, 3.398 mmol) which was dissolved in methanol (40 mL) forming a clear colourless solution. A second solution containing nickel chloride hexahydrate ($NiCl_2{\cdot}6H_2O$, 0.424 g, 1.699 mmol) in deionised water (20 mL) was prepared giving a clear green solution. The nickel solution was added to that of the dithiophosphonato ligand while stirring over a period of 5 minutes, this resulted in the formation of copious amounts of purple precipitate indicating the formation of the nickel complex. The precipitate was collected by vacuum filtration, washed by water (3 x

10 mL) and allowed to dry under vacuum for a period of 3 hours, yielding a purple powder (0.740 g, 30% yield). Purple crystals suitable for X-ray analysis were grown by vapour diffusion of hexane (8 mL) into a dichloromethane solution of the complex (0.270 g, 0.443 mmol in 4 mL). Melting point at 122 - 123°C. Elemental % composition found (analytical calculation for $C_{22}H_{32}O_4P_2S_4Ni$) : C 44.25 (43.36), H 5.50 (5.29).

^{31}P NMR ($CDCl_3$): δ (ppm): 101.27. ^{1}H NMR ($CDCl_3$): δ (ppm): 7.95 (2H, dd, J(^{31}P-^{1}H) = 13.96 Hz, J(^{1}H -^{1}H) =8.80 Hz, *ortho*-ArH) , 6.94 (2H, dd, J(^{31}P-^{1}H) = 8.82 Hz, J(^{1}H -^{1}H) =3.06 Hz, *meta*-ArH), 4.26 (2H, dot, J(^{1}H -^{1}H) = 7.89 Hz, $POCH_2$), 4.06 (2H, q, J(^{1}H-^{1}H)=6.97 Hz, $ArOCH_2$), 1.74 (2H, m, J(^{1}H -^{1}H) = 7.16 Hz, $POCH_2CH_2$), 1.41 (3H, t, J(^{1}H -^{1}H) = 6.98 Hz, $ArOCH_2CH_3$), 0.96 (3H, t, J(^{1}H -^{1}H) = 7.38 Hz, $POCH_2CH_2CH_3$). ^{13}C NMR ($CDCl_3$): δ (ppm): 162.37 (*para*-ArC), 131.73 (*meta*-ArC), 128.97 (*ipso*-ArC), 114.40 (*ortho*-ArC), 67.89 ($POCH_2$), 63.77 ($ArOCH_2$), 23.58 ($POCH_2CH_2$), 14.85 ($ArOCH_2CH_3$), 10.27 ($POCH_2CH_2CH_3$).

Selected IR data *v*/cm^{-1}: 1179 (m), 1042(m), 685 (s), 565 (s)

2.6.4 Synthesis of $Ni[S_2P(4\text{-}C_6H_4OEt)(OCH(CH_3)CH_2CH_3)]_2$ (4A)

A beaker was charged with $(NH_4)[S_2P(4\text{-}C_6H_4OEt)(OCH(CH_3)CH_2CH_3)]$ (1.000 g, 3.347 mmol) which was dissolved in methanol (40 mL) forming a clear colourless solution. A second solution containing nickel chloride hexahydrate ($NiCl_2{\cdot}6H_2O$, 0.387 g, 1.626 mmol) in deionised water (20 mL) was prepared giving a clear green solution. The nickel solution was added to that of the dithiophosphonate while stirring over a period of 5 minutes, this resulted in the formation of copious amounts of purple precipitate indicating the formation of the desired complex. The precipitate was collected by vacuum filtration on a Buchner funnel, washed by water (3 x 10 mL) and allowed to dry under vacuum for a period of 3 hours,

yielding a crystalline purple powder (0.922 g, 72% yield). Purple crystals suitable for X-ray analysis were grown by vapour diffusion of hexane (8 mL) into a dichloromethane solution of the $Ni[S_2P(4\text{-}C_6H_4OEt)(OCH(CH_3)CH_2CH_3)]_2$ (0.305 g, 0.388 mmol in 4 mL). Melting point: 156-157 °C. Elemental % composition found (analytical calculation for $C_{24}H_{36}O_4P_2S_4Ni$) : C 44.96 (45.22), H 5.91 (5.69).

^{31}P NMR ($CDCl_3$): δ (ppm): 97.99. ^{1}H NMR ($CDCl_3$): δ (ppm): 7.99 (2H, dd, $J(^{31}P\text{-}^{1}H)$ = 13.96 Hz, $J(^{1}H\text{-}^{1}H)$ = 8.68 Hz, *ortho*-ArH) , 6.96 (2H, dd, $J(^{31}P\text{-}^{1}H)$ = 8.76 Hz, $J(^{1}H\text{-}^{1}H)$ = 3.12 Hz, *meta*-ArH), 4.99 (1H, d quart, $J(^{31}P\text{-}^{1}H)$ = 26.51 Hz, $J(^{1}H\text{-}^{1}H)$ = 6.17 Hz, CH), 4.08 (2H, quart, $J(^{1}H\text{-}^{1}H)$ = 6.99 Hz, $ArOCH_2$), 1.69 (2H, m, $J(^{1}H\text{-}^{1}H)$ = 7.32 Hz, $OCH(CH_3)\mathbf{CH_2}CH_3$) 1.43 (3H, t, $J(^{1}H\text{-}^{1}H)$ = 6.96 Hz, $ArOCH_2CH_3$), 1.40 (3H, d, $J(^{1}H\text{-}^{1}H)$ = 6.52 Hz, $OCH(\mathbf{CH_3})CH_2CH_3$), 0.96 (3H, t, $J(^{1}H\text{-}^{1}H)$ = 7.46 Hz, $OCH(CH_3)CH_2\mathbf{CH_3}$) . ^{13}C NMR ($CDCl_3$): δ (ppm): 162.17 (*para*-ArC), 131.72 (*meta*-ArC), 129.39 (*ipso*-ArC), 114.28 (*ortho*-ArC), Peak masked due to solvent (CH), 63.75 ($ArOCH_2$), 30.54 ($OCH(CH_3)\mathbf{CH_2}CH_3$), 21.80 ($OCH(\mathbf{CH_3})CH_2CH_3$), 14.67 ($ArOCH_2CH_3$), 9.62 ($OCH(CH_3)CH_2\mathbf{CH_3}$).

Selected IR data ν/cm^{-1}: 1180 (m), 1045(m), 684 (s), 560 (s)

2.6.5 Synthesis of $Ni[S_2P(4\text{-}C_6H_4OEt)(OCH(CH_3)CH_2CH_3)(tbp)]_2$ (4Ai)

A Schlenk flask was charged with $Ni[S_2P(4\text{-}C_6H_4OEt)(OCH(CH_3)CH_2CH_3)]_2$ (0.182 g, 0.286 mmol). The complex was dissolved in 30 mL of toluene, forming a clear purple solution. A solution containing 4-tert-butyl pyridine (0.077 g, 0.571 mmol) in toluene (20 mL) was added drop wise to the Schlenk flask over a period of 5 minutes with constant stirring. The reaction mixture gradually changed from purple to brown and eventually to green. After a further 5 minutes the solution began to form a pale green precipitate. The precipitate was removed by

gravity filtration and the filtrate allowed to slowly evaporate in a partially covered 100 mL beaker for a period of 5 days, yielding green crystals suitable for X-ray analysis. Yield (filtered precipitate + dry product, including crystals) = 0.231 g, 89 %. Colour transition from green to purple at 164 °C, melting point 185 °C. Elemental % composition found (analytical calculation for $C_{42}H_{62}N_2O_4P_4S_4Ni$) : C 56.20 (55.57), H 6.10 (6.88), N 2.94 (3.09).

Selected IR data ν/cm^{-1}: 1175 (m), 677 (s), 562 (s), 426 (w)

2.7 Mercury Complexes

2.7.1 Synthesis of $Hg_2[S_2P(4\text{-}C_6H_4OEt)(OCH_3)]_4$ (1B)

A beaker was charged with $(NH_4)[S_2P(4\text{-}C_6H_4OEt)(OCH_3)]$ (1.202 g, 4.530 mmol) which was then dissolved in methanol (40 mL) forming a clear colourless solution. A second solution containing mercury nitrate monohydrate ($Hg(NO_3)_2{\cdot}H_2O$, 0.788 g, 2.301 mmol) in deionised water (20 mL) was prepared giving a clear colourless solution. The mercury solution was added to that of the dithiophosphonato ligand while stirring over a period of 5 minutes, the solution began to form a sticky off-white to yellow solid. The reaction mixture was heated to a temperature of 70 °C for a further 5 minutes, in order to facilitate complete complexation. This resulted in the formation of a fine white precipitate in addition to the initially formed solid. The solids were collected by vacuum filtration, washed with water (3 x 10 mL) and allowed to dry under vacuum for a period of 6 hours, yielding an off-white solid (0.982 g, 31% yield). Colourless crystals suitable for X-ray analysis were grown by vapour diffusion of hexane (8 mL) into a dichloromethane solution of the complex (0.302 g, 0.217 mmol in 4 mL). The resulting crystals of **1B** were found to decompose at temperatures exceeding 120 °C. Elemental % composition found (analytical calculation for $C_{36}H_{48}O_8P_4S_8Hg_2$) : C 31.81 (31.10), H 3.28 (3.48).

^{31}P NMR ($CDCl_3$): δ (ppm): 105.97. ^{1}H NMR ($CDCl_3$): δ (ppm): 7.94 (2H, dd, J(^{31}P-^{1}H) = 14.52 Hz, J(^{1}H -^{1}H) = 8.84 Hz, *ortho*-ArH) , 6.93 (2H, dd, J(^{31}P-^{1}H) = 8.80 Hz, J(^{1}H -^{1}H) =3.40 Hz, *meta*-ArH), 4.06 (2H, quart, J(^{1}H -^{1}H) = 7.00 Hz, $ArOCH_2$), 3.97 (3H, d, J(^{31}P-^{1}H)=15.6 Hz, CH_3), 1.41 (3H, t, J(^{1}H -^{1}H) = 6.96 Hz, $ArOCH_2CH_3$). ^{13}C NMR ($CDCl_3$): δ (ppm): 162.26 (*para*-ArC), 132.08 (*meta*-ArC), 128.62 (*ipso*-ArC), 114.42 (*ortho*-ArC), 63.73 ($ArOCH_2$), 52.62 (CH_3), 14.57 ($ArOCH_2CH_3$).

Selected IR data *v*/cm^{-1}: 1176 (m), 1015(m), 679 (s), 543 (s)

2.7.2 Synthesis of $Hg_2[S_2P(4\text{-}C_6H_4OEt)(OCH(CH_3)_2)]_4$ (2B)[12]

A beaker was charged with $(NH_4)[S_2P(4\text{-}C_6H_4OEt)(OCH(CH_3)_2)]$ (1.322 g, 4.506 mmol) and dissolved in methanol (40 mL) forming a clear colourless solution. A second solution containing mercury nitrate monohydrate ($Hg(NO_3)_2{\cdot}H_2O$, 0.772 g, 2.253 mmol) in deionised water (20 mL) was prepared, also giving a clear colourless solution. The mercury solution was added to that of the dithiophosphonato ligand while stirring over a period of 5 minutes, this resulted in the formation of copious amounts of white precipitate indicating the formation of the desired complex. The precipitate was collected by vacuum filtration, washed with water (3 x 10 mL) and allowed to dry under vacuum for a period of 3 hours, yielding a crystalline off white to pale yellow powder (0.720 g, 43 % yield). Colourless crystals suitable for X-ray analysis were grown by vapour diffusion of hexane (8 mL) into a dichloromethane solution of $Hg_2[S_2P(4\text{-}C_6H_4OEt)(OCH(CH_3)_2)]_4$ (0.3 g, 0.399 mmol in 4 mL). Melting point of 117 - 118 °C. Elemental % composition found (analytical calculation for $C_{44}H_{64}O_8P_4S_8Hg_2$) : C 34.80 (35.17), H 4.02 (4.29).

^{31}P NMR ($CDCl_3$): δ (ppm): 100.73. ^{1}H NMR ($CDCl_3$): δ (ppm): 7.93 (2H, dd, J(^{31}P-^{1}H) = 14.46 Hz, J(^{1}H -^{1}H) = 8.82 Hz, *ortho*-ArH) , 6.91 (2H, dd, J(^{31}P-^{1}H) = 8.84 Hz, J(^{1}H -^{1}H) =

3.40 Hz, *meta*-ArH), 5.23 (1H, d quart, J(^{31}P-^{1}H) = 20.82 Hz, J(^{1}H -^{1}H) = 6.19 Hz, CH), 4.05 (2H, quart, J(^{1}H -^{1}H) = 6.96 Hz, $ArOCH_2$), 1.42 (6H, d, J(^{1}H -^{1}H) = 6.2 Hz, CH_3), 1.39 (3H, t, J(^{1}H -^{1}H) = 6.96 Hz, $ArOCH_2CH_3$). ^{13}C NMR ($CDCl_3$): δ (ppm): 162.27 (*para*-ArC), 132.15 (*meta*-ArC), 130.40 (*ipso*-ArC), 114.32 (*ortho*-ArC), 72.22 (CH), 64.03 ($ArOCH_2$), 24.27 (CH_3), 14.91 ($ArOCH_2CH_3$).

Selected IR data *v*/cm^{-1}: 1181 (m), 1043(m), 685 (s), 534 (s)

2.8 A Cadmium Complex

2.8.1 Synthesis of $Cd_2[S_2P(4\text{-}C_6H_4OEt)(OCH_3)]_4$ (1C)

A beaker was charged with $(NH_4)[S_2P(4\text{-}C_6H_4OEt)(OCH_3)]$ (1.020 g, 3.844 mmol) which was dissolved in methanol (40 mL) forming a clear colourless solution. A second solution containing cadmium nitrate tetrahydrate ($Cd(NO_3)_2{\cdot}4H_2O$, 0.603 g, 1.956 mmol) in deionised water (20 mL) was prepared giving a clear colourless solution. The cadmium solution was added to that of the dithiophosphonato ligand while stirring over a period of 5 minutes, this resulted in the formation of a pure white precipitate indicating the formation of the cadmium complex. The precipitate was collected by vacuum filtration, washed with water (3 x 10 mL) and allowed to dry under vacuum for a period of 3 hours, yielding a white powder (1.086 g, 47% yield). Colourless crystals suitable for X-ray analysis were grown by vapour diffusion of hexane (8 mL) into a dichloromethane solution of the complex (0.302 g, 0.217 mmol in 4 mL). Melting point: 157 °C. Elemental % composition found (analytical calculation for $C_{36}H_{48}O_8P_4S_8Cd_2$) : C 36.45 (35.62), H 4.19 (3.99).

^{31}P NMR ($CDCl_3$): δ (ppm): 108.59. ^{1}H NMR ($CDCl_3$): δ (ppm): 7.95 (2H, dd, J(^{31}P-^{1}H) = 14.58 Hz, J(^{1}H -^{1}H) = 8.70 Hz, *ortho*-ArH) , 6.90 (2H, dd, J(^{31}P-^{1}H) = 8.78 Hz, J(^{1}H -^{1}H)

=3.26 Hz, *meta*-ArH), 4.04 (2H, quart, J(^{1}H -^{1}H) = 6.97 Hz, $ArOCH_2$), 3.81 (3H, d, J(^{31}P-^{1}H)=15.48 Hz, CH_3), 1.40 (3H, t, J(^{1}H -^{1}H) = 6.96 Hz, $ArOCH_2CH_3$). ^{13}C NMR ($CDCl_3$): δ (ppm): 162.32 (*para*-ArC), 132.65 (*meta*-ArC), 128.48 (*ipso*-ArC), 114.62 (*ortho*-ArC), 63.98 ($ArOCH_2$), 53.11 (CH_3), 14.87 ($ArOCH_2CH_3$).

Selected IR data *v*/cm^{-1}: 1176 (m), 1016(m), 651 (s), 550 (s)

2.9 A Lead Complex

2.9.1 Synthesis of $Pb[S_2P(4\text{-}C_6H_4OEt)(OCH(CH_3)_2)]_2$ (2D)[13]

A beaker was charged with $(NH_4)[S_2P(4\text{-}C_6H_4OEt)(OCH(CH_3)_2)]$ (1.010 g, 3.443 mmol) and dissolved in methanol (40 mL) forming a clear colourless solution. A second solution containing lead nitrate ($Pb(NO_3)_2$, 0.570 g, 1.721 mmol) in deionised water (20 mL) was prepared also giving a clear colourless solution. The lead solution was added to that of the dithiophosphonato ligand while stirring over a period of 5 minutes, this resulted in the formation of copious amounts of off-white precipitate. The precipitate was collected by vacuum filtration, washed by water (3 x 10 mL) and allowed to dry under vacuum for a period of three hours, yielding an off white powder (0.926 g, 71 % yield). Clear crystals suitable for X-ray analysis were grown by vapour diffusion of hexane (8 mL) into a dichloromethane solution of complex **2D** (0.3 g, 0.396 mmol in 4 mL). Melting point: 129-130 °C. Elemental % composition found (analytical calculation for $C_{22}H_{32}O_4P_2S_4Pb$) : C 35.16 (34.86), H 4.05 (4.26).

^{31}P NMR ($CDCl_3$): δ (ppm): 94.20. ^{1}H NMR ($CDCl_3$): δ (ppm): 7.89(2H, dd, J(^{31}P-^{1}H) = 14.5 Hz, J(^{1}H -^{1}H) = 8.74 Hz, *ortho*-ArH) , 6.89(2H, dd, J(^{31}P-^{1}H) = 8.74 Hz, J(^{1}H -^{1}H) = 3.22 Hz, *meta*-ArH), 5.01(1H, d quart, J(^{31}P-^{1}H) = 21.35 Hz, J(^{1}H -^{1}H) = 6.18 Hz, CH), 4.03(2H,

quart, J(^{1}H -^{1}H) = 6.97 Hz, $ArOCH_2$), 1.39(3H, t, J(^{1}H -^{1}H) = 6.98 Hz, $ArOCH_2CH_3$), 1.32(6H, d, J(^{1}H -^{1}H) = 6.16 Hz, CH_3). ^{13}C NMR ($CDCl_3$): δ (ppm): 161.97 (*para*-ArC), 133.32 (*ipso*-ArC), 131.57 (*meta*-ArC), 114.32 (*ortho*-ArC), 71.34 (CH), 64.03($ArOCH_2$), 24.85 (CH_3), 14.91 ($ArOCH_2CH_3$).

Selected IR data v/cm^{-1}: 1178 (m), 1044(m), 679 (s), 542 (s)

2.10 References

1. Nonius, Delft, The Netherlands, 1998.
2. Z. Otwinowski and W. Minor, *Methods in enzymology, macromolecular Crystallography*, Part:A edn., Academic Press, 1997.
3. G. Sheldrick, SADABS, University of Gottingen, Germany, 1996.
4. Bruker, Bruker AXS Inc., Madison, Wisconsin, USA, 2007.
5. G. Sheldrick, *Acta Crystallogr. Sect. A*, 2008, **64**, 112-122.
6. C. Barnes, *J. Appl. Crystallogr.*, 1997, **30**, 568.
7. C. F. Macrae, P. R. Edgington, P. McCabe, E. Pidcock, G. P. Shields, R. Taylor, M. Towler and J. van de Streek, *J. Appl. Crystallogr.*, 2006, **39**, 453-457.
8. W. E. Van Zyl and J. P. Fackler, *Phosphorus, Sulfur Silicon Relat. Elem.*, 2000, **167**, 117-132.
9. S. Sewpersad, B. Omondi and W. E. Van Zyl, *Acta Crystallogr., Sect. E: Struct.*, 2012, **68**, m1483.
10. S. Sewpersad and W. E. Van Zyl, *Acta Crystallogr., Sect. E: Struct.*, 2012, **68**, m1457.
11. S. Sewpersad, B. Omondi and W. E. Van Zyl, *Acta Crystallogr., Sect. E: Struct.*, 2012, **68**, m1534.
12. S. Sewpersad and W. E. Van Zyl, *Acta Crystallogr., Sect. E: Struct.*, 2012, **68**, m1488-m1489.
13. S. Sewpersad and W. E. Van Zyl, *Acta Crystallogr., Sect. E: Struct.*, 2012, **68**, m1502.

Chapter 3: Neutral mononuclear Ni(II) dithiophosphonato complexes

3.1 Dithiophosphonate Salts

The complexes synthesized in the present study are based on four distinct ligands (**1-4**), all derived from the phenetole Lawesson's reagent dimer C (**Figure 1.1**) and its subsequent reactions with the primary and secondary alkyl alcohols methanol (**1**), 2-propanol (**2**), 1-propanol (**3**) and 2-butanol (**4**). Complexes of Ni(II) (**A**), Hg(II) (**B**), Cd(II) (**C**) and Pb(II) (**D**) were prepared.

3.1.1 Preparation

The synthetic methodology (**Scheme 3.1**) for ligand preparation proved facile and was carried out as described in literature.[1] Two stoichiometric equivalents of the relevant alcohol were added to phenetole Lawesson's reagent dimer and heated to temperatures not exceeding 80 °C. The mixture was allowed to react until the suspension became clear, thereby indicating the successful cleavage of the diphosphetane disulfide dimer and resultant formation of the dithiophosphonic acid. It is worth noting that no additional solvent was required and thus the synthesis of the dithiophosphonic acids fall in the category of "green chemistry". Once cooled, the acid was readily deprotonated by bubbling ammonia gas through the reaction mixture resulting in the formation of white solids, indicating the formation of the respective ammonia salt of the parent dithiophosphonic acid. Isolation and workup of each salt was relatively simple, involving stirring in diethyl ether, and additional bubbling of ammonia. Products were dried under reduced pressure, and ligands **1**, **2** and **4** were all isolated as fine white powders within 4 hours of the start of synthesis while

compound **3** required overnight stirring before a powder of suitable quality could be obtained. All ligands were obtained in essentially quantitative yields, see **Table 3.2**.

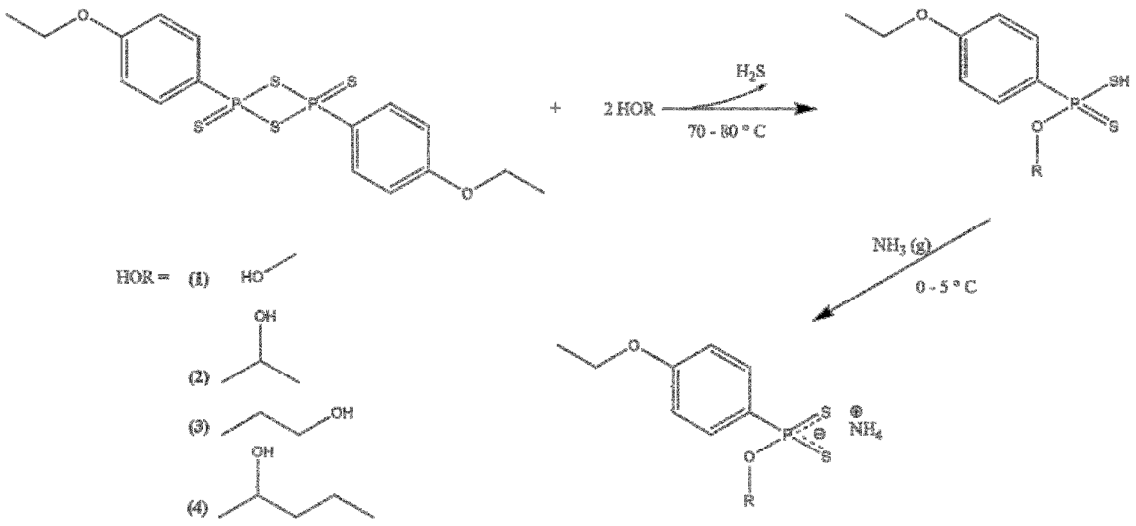

Scheme 3.1: Synthetic route from phenetole Lawesson's reagent to compounds 1-4

3.1.2 Characterization

Full elucidation by solution NMR spectroscopy (^{1}H, ^{31}P and ^{13}C) was conducted in methanol-d_4 as the ammonium dithiophosphonate salts proved insoluble in $CDCl_3$. The ^{31}P NMR spectra were vital when assessing whether the desired product was formed and in each case the spectrum provided a sharp singlet, indicating the formation of a single phosphorus bearing product, the peaks for the ligand salts ranged from 104 to 109 ppm, consistent with the shift range of 90-112 ppm reported for similar dithiophosphonate products (see **Table 3.1**).[1] The ^{1}H and ^{13}C NMR spectra of the salts were consistent with the presence of both phenetyl and the respective alkoxy moieties, see **Chapter 2**.

Infrared spectra of the dithiophosphonate salts show distinct bands at 1043-1040 cm^{-1}, 1028-1025 cm^{-1}, 674-666 cm^{-1} and 565-556 cm^{-1}, corresponding to ν[(P)–O–C], ν[P–O–(C)], $\nu(PS)_{asym}$ and $\nu(PS)_{sym}$ stretches, respectively.[2] The broad bands between 3300-2800 cm^{-1} corresponded to the N-H stretching bands and provided an indication that an ammonium salt

was present.[3] Melting point analysis was also carried out and sharp melting point ranges in each case were obtained, signifying high bulk purity (**Table 3.1**). Further proof of ligand formation was afforded by the subsequent complexation reactions of each ligand and X-ray crystallographic studies of the metal complexes

Table 3.1: Characterization data of compounds 1-4

Ligand	Parent Alcohol	Melting point / °C	Yield / %	^{31}P NMR shift / ppm
1	methanol	162	74	109
2	2-propanol	184 - 185	85	104
3	1-propanol	148 - 150	88	107
4	2-butanol	135 - 136	85	105
Phenetole L.R		214-215 decomp.	-	insoluble in deuterated solvents available

The above characterization results were deemed satisfactory in confirming that the desired ligands had been synthesised and were suitable for use in subsequent complexation reactions.

3.2 New Nickel(II) Dithiophosphonate Complexes

Of all the dithiophosphonate complexes and crystal structures reported in literature, those of nickel(II) are most dominant,[4-9] presumably due to the ease of both complex formation and subsequent crystal growth. Four new neutral Ni(II) dithiophosphonate complexes (**1A,**[10] **2A**,[11] **3A**,[12] **4A**) were synthesized and their respective crystal structures reported in the present study, along with a novel octahedral nickel complex (**4Ai**) comprising a secondary ligand, 4-tert-butyl pyridine, as an adduct to complex **4A**.

3.2.1 Complex Preparation

An interesting feature of the complexation reactions is that they may be carried out in partially aqueous conditions, usually in methanolic media regardless of the ligand used, water was added to the reaction mixture not only to dissolve the metal salt, but also to force the precipitation of the formed complex, while also ensuring complete dissolution, and thus removal, of any ionic by-products (ammonium chloride or ammonium nitrate, depending on the metal salt used) in the filtration step. While tolerant of such conditions, the reaction time was relatively short in duration, ensuring no side products or unwanted oxidation products were formed from reactions between the ligand used and the reaction media. The complexes synthesized in this study were formed in aqueous media. Aqueous reaction conditions should be avoided in cases where the metal salt is susceptible to reduction or oxidation of the metal *i.e.* Au(I) and Cu(I) salts, in such cases complexation is carried out under inert conditions in media such as tetrahydrofuran or acetonitrile.[13]

Complexes **1A**, **2A**, **3A**, **4A** were produced in the same general manner. Two stoichiometric equivalents of the respective dithiophosphonate salt (**1-4**) were dissolved in methanol, while one stoichiometric equivalent of the green Ni(II) salt ($NiCl_2 \cdot 6H_2O$) was dissolved in water. Evolution of a purple precipitate was observed upon addition of the solutions indicating product formation, the colour change was also indicative of the transition from a 6-coordinate to 4-coordinate Ni(II) system. Solid products were easily isolated by filtration, as the ammonium chloride by-product was extracted into the aqueous reaction media. All crystals were grown by slow diffusion of hexane into a DCM solution of the respective complex, all were purple in colour.

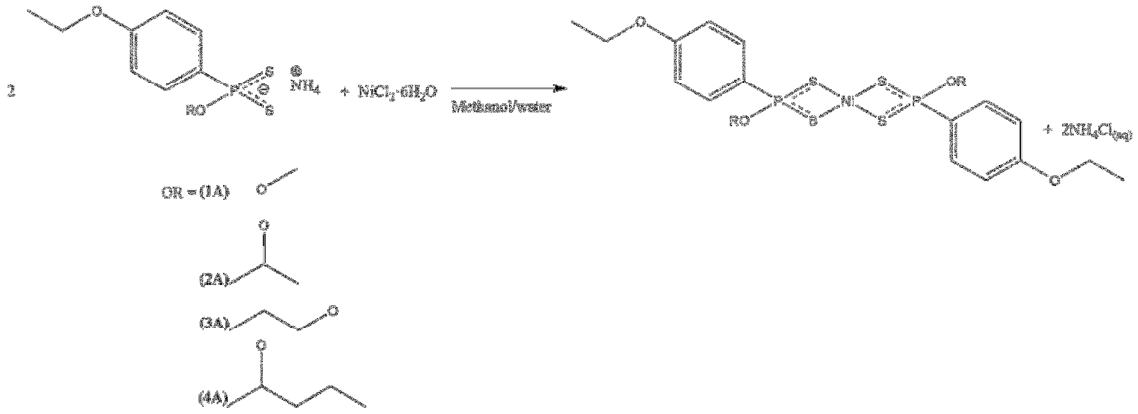

Scheme 3.2: Preparation of new Ni(II) dithiophosphonato complexes

3.2.2 Characterization

The secondary alcohol based complexes, **2A** and **4A** were isolated in high yields, 75 and 72%, respectively, while complexes **1A** and **3A**, both derived from primary alcohol based ligands, had significantly lower yields, 41 and 30%, respectively. This was due to an increased stability of the secondary alcohol-based ligands in aqueous solution when compared to those of the primary species, which were more susceptible to side reactions with the reaction media. The primary alcohol ligands were thus deemed to have been subjected to competition between complexation reactions, which form aqueous stable metal chelates and hydrolysis reactions of the ligands, resulting in the reduced yields of these complexes.

Each of the Ni(II) complexes had sharp melting points indicating that the products formed were relatively pure, the melting point temperatures of the respective Ni(II) complexes were significantly higher than those of the analogous metal complexes reported in this study, clearly illustrating the greater ionic nature of the Ni(II) complexes, when compared to the other metals used in this study.[14] Infrared spectra of the complexes formed were consistent with data previously discussed for the ligand IR assignment (**3.1.2**), a notable feature of the complex IR spectra, however, was the disappearance of the broad N-H stretching bands

associated with the dithiophosphonate salt, indicating removal of the ammonium ion and thus binding of the ligand to the metal nucleus.

The Ni(II) dithiophosphonate complexes were all subjected to solution NMR examination (^{1}H, ^{31}P and ^{13}C) in $CDCl_3$. The complexes, unlike their respective parent ligands, were readily soluble in deuterated chloroform. The ^{1}H and ^{13}C spectra confirmed the presence of the phenetyl and respective alkoxy groups. The ^{31}P spectra of each of the complexes showed sharp singlets, indicating presence of equivalent P atoms within the complexes, see **Table 3.2**. It should also be pointed out that each Ni(II) complex can, in principle, also form a *cis* isomer for which a second singlet peak would be expected in close proximity to the *trans* isomer which formed exclusively in the solid state. Since no second singlet peak was observed, it was concluded that the *cis* isomer either did not form in solution, or the cis/trans isomerization barrier was too high to be detected on the NMR timescale. Variable temperature (VT) NMR, coupled with theoretical calculations could be considered in future to resolve this issue, but such investigations fell outside the scope of the present study. In each case elemental analysis was consistent with calculated data (see **Chapter 2**).

Table 3.2: Characterization data of Ni(II) dithiophosphonate complexes synthesized

Complex	Ligand Alkoxy Group	Melting point / °C	Yield / %	^{31}P NMR shift / ppm
1A	methoxy	168	41	105
2A	2-propoxy	168-169	75	98
3A	1-propoxy	122 - 123	30	101
4A	2-butoxy	156-157	72	98

3.2.3 Crystallographic studies

The molecular solid state structures of complexes **1A**, **2A**, **3A** and **4A** are all mononuclear, comprising of two ligands bonded to a single Ni(II) centre, resulting in the formation of

chelating NiS_2P rings. The 4-coordinate Ni atom was found to adopt distorted square planar geometries, thus showing a preference for resonance structure L (**Figure 1.3**) consistent with previously reported Ni(II) complexes in the phosphor-1,1-dithiolate class of ligands.[15] Nickel dithiophosphonate complexes within this dissertation have been described by employing *cis* and *trans* terminology, denoting stereochemistry of similar groups about the central Ni atom. In each of the Nickel (II) dithiophosphonate complexes studied, the phenetyl and alkoxy groups of one ligand were found to be held *trans* to the respective equivalent groups of the other chelating ligand. Thus a centre of inversion was found to exist at the Ni(II) nucleus in all the respective complexes.

In the **Figures 3.1, 3.4, 3.6** and **3.8**, the nickel nuclei as well as the ligands are clearly shown to behave as described above. The ligands bind in an isobidentate manner, illustrated by the equivalent bond lengths of all the P-S bonds present, ca. 2.00 Å, see **Tables 3.2.2 - 3.2.5**. The Ni-S bond distances in all the Ni(II) complexes synthesized are approximately equi-distant at *ca*. 2.2 Å. The distorted square planar geometries are confirmed by the S-Ni-S bond angles of the asymmetric unit, *ca* 88 °. The Ni atom adopts binding mode Q (**Figure 1.4**). This confirms the preference of Nickel(II) for resonance structure L (**Figure 1.3**), in which delocalization of the P-S π bond occurs, evenly distributing electron density over the S-P-S moiety. The S-P-S bite angles range from 101° to 102°.

The crystal structure of **4A** (**Figure 3.7**), unlike the other nickel(II) complexes, shows disorder in the resolution of the alkoxy group (2-butoxy), the O1 atom as well as the C atoms of the alkyl chain are all disordered denoted on the structure diagram by 'a' and 'b' labels on the structure diagram. The reason for this disorder was due to the 'flapping' motion of the longer alkyl chain which is not sufficiently negated at the data collection temperature of 173K.

In **Figures 3.2** and **3.7** the crystallographic packing of complexes **1A** (similar to the Mercury(II) (**1B**) and Cadmium(II) (**1C**) complexes) and **3A** are presented. These complexes pack in the monoclinic system in centrosymmetric space group P21/c.[16] **Figures 3.5** and **3.7** show the crystallographic packing of complexes **2A** and **4A** respectively, both adopt the triclinic crystal system in centrosymmetric space group P-1.[16] Upon examination of data represented in **Table 3.7** it is clear that crystal density decreases with an increase in the length of the alkyl chain of the alcohol group. Thus it can be stated that **1A** exihibits the highest crystal packing efficiency, while **4A** packs least efficiently. It was also clearly evident that the degree of substitution of the ligand alkyl groups had an impact on the volume of the unit cell. From **Table 3.7** it can be seen that the secondary alcohol complexes **2A** [695.22(10) $Å^3$] and **4A** [757.72(3) $Å^3$] both had significantly lower unit cell volumes than the primary alcohol complexes **1A [**1160.74(7) $Å^3$]and **3A** [1369.54(5) $Å^3$].

Complex **1A** differs from other structures in that intermolecular S-S interactions are present, one S atom of a molecular unit is shown to interact with two S atoms of a neighbouring molecular unit, shown in **Figure 3.3**. The intermolecular S-S interaction distances are 3.561(5) Å and 3.337(5) Å. The presence of this unique interaction in **1A** is attributed to the much shorter nature of the alkoxy chain in this case, thus lack of this interaction in complexes **2A, 3A** and **4A**, due to steric reasons.

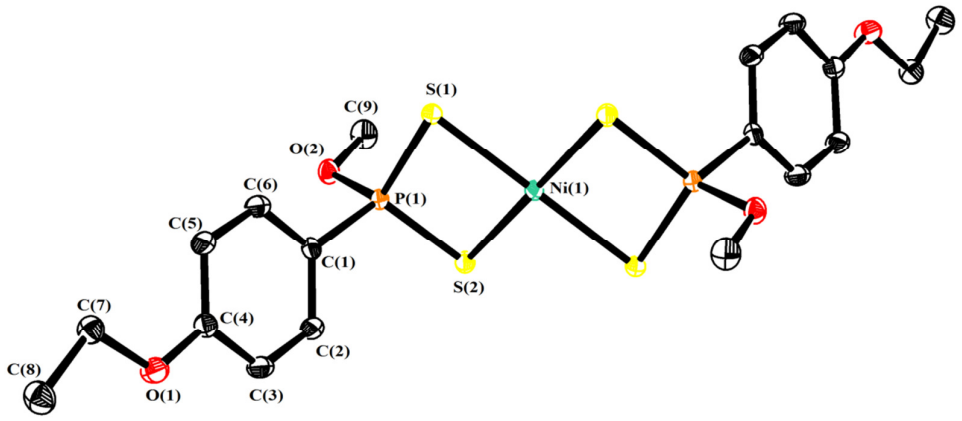

Figure 3.1: Molecular structure of complex 1A. ORTEP diagram, thermal ellipsoids drawn at 50% probability, symmetric ellipsoids were generated by symmetry code 2-x, 2-y, 2-z and have not been labelled. Hydrogen atoms are omitted for clarity.

Table 3.3: Selected bond lengths (Å) and angles (°) for 1A

O(2)-P(1)	1.5902(10)	C(9)-O(2)-P(1)	118.47(9)
P(1)-S(2)	1.9996(5)	O(2)-P(1)-C(1)	101.76(6)
P(1)-S(1)	2.0061(5)	O(2)-P(1)-S(2)	113.60(4)
P(1)-Ni(1)	2.8306(4)	C(1)-P(1)-S(2)	113.88(5)
S(1)-Ni(1)	2.2455(3)	O(2)-P(1)-S(1)	113.49(4)
S(2)-Ni(1)	2.2328(4)	C(1)-P(1)-S(1)	112.10(5)
		S(2)-P(1)-S(1)	102.47(2)
		O(2)-P(1)-Ni(1)	138.74(4)
		C(1)-P(1)-Ni(1)	119.49(5)
		S(2)-P(1)-Ni(1)	51.639(13)
		S(1)-P(1)-Ni(1)	51.985(12)
		P(1)-S(1)-Ni(1)	83.279(16)
		P(1)-S(2)-Ni(1)	83.755(17)
		S(2)-Ni(1)-S(1)	88.443(13)
		S(2)-Ni(1)-P(1)	44.606(11)

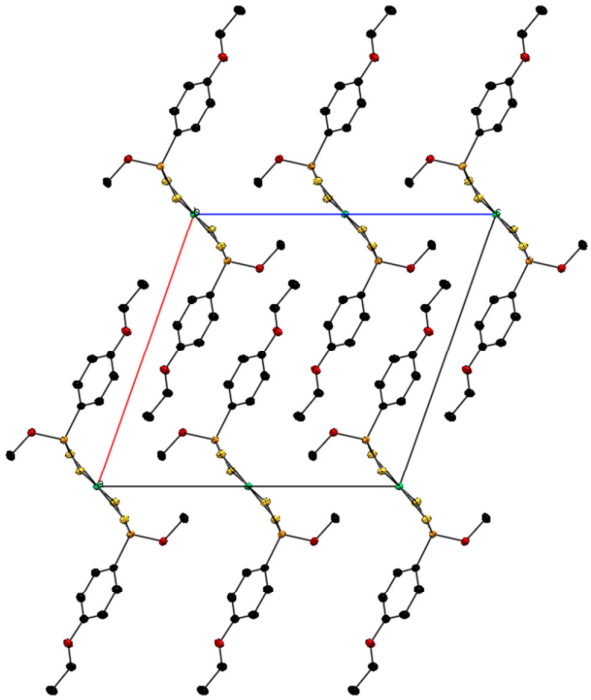

Figure 3.2: Packing of complex 1A viewed along the b axis. Hydrogen atoms have been omitted for clarity.

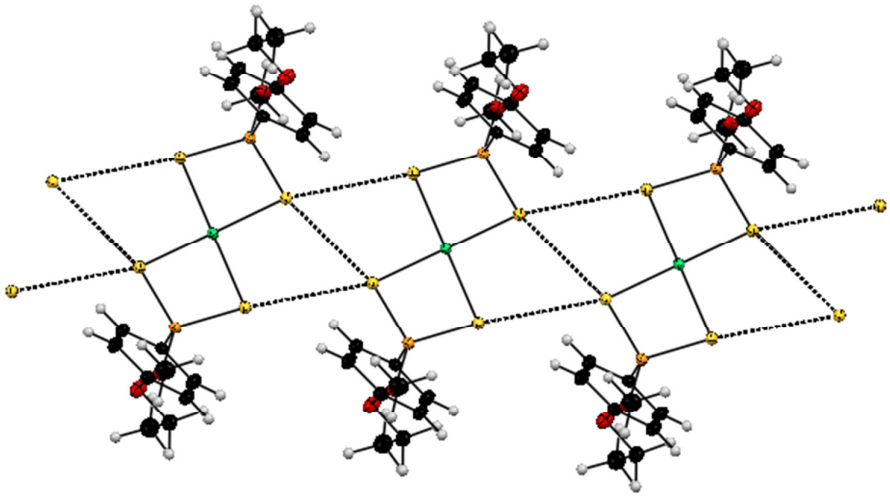

Figure 3.3: Intermolecular S-S interactions present in complex 1A

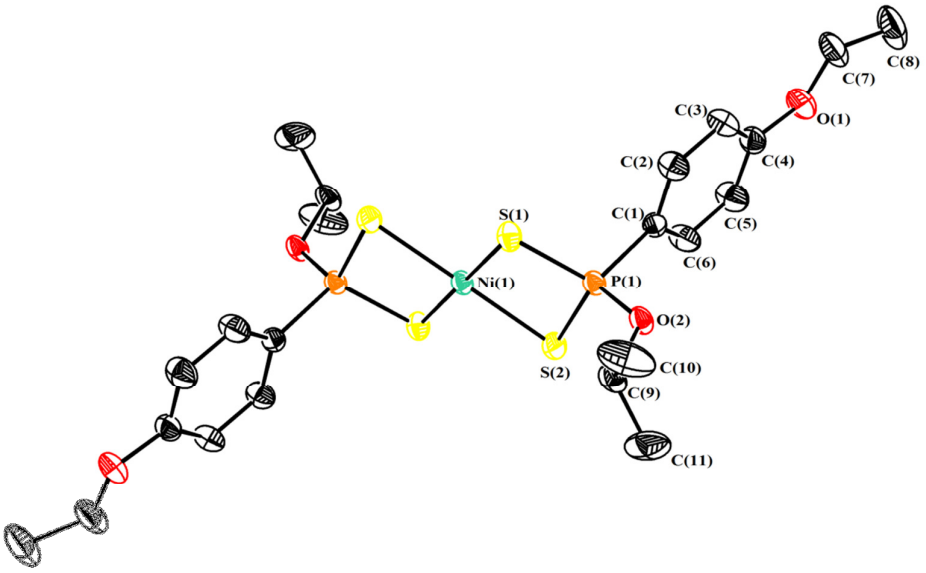

Figure 3.4: Molecular structure of complex 2A. ORTEP diagram, thermal ellipsoids drawn at 50% probability, symmetric ellipsoids were generated by symmetry code 1-x, 1-y, -z and have not been labelled. Hydrogen atoms are omitted for clarity.

Table 3.4: Selected bond lengths (Å) and angles (°) for 2A

O(2)-P(1)	1.5828(14)	C(9)-O(2)-P(1)	121.36(12)
P(1)-S(2)	2.0053(8)	O(2)-P(1)-C(1)	100.71(8)
P(1)-S(1)	2.0036(8)	O(2)-P(1)-S(2)	114.16(6)
P(1)-Ni(1)	2.8224(6)	C(1)-P(1)-S(2)	113.46(6)
S(1)-Ni(1)	2.2369(6)	O(2)-P(1)-S(1)	113.76(6)
S(2)-Ni(1)	2.2328(6)	C(1)-P(1)-S(1)	113.39(6)
Ni(1)-S(2)^{i}	2.2328(6)	S(2)-P(1)-S(1)	101.93(3)
Ni(1)-S(1)^{i}	2.2369(6)	O(2)-P(1)-Ni(1)	141.40(6)
Ni(1)-P(1)^{i}	2.8224(6)	C(1)-P(1)-Ni(1)	117.89(6)
		S(2)-P(1)-Ni(1)	51.79(2)
		S(1)-P(1)-Ni(1)	51.91(2)
		P(1)-S(1)-Ni(1)	83.26(3)
		P(1)-S(2)-Ni(1)	83.33(2)
		S(2)-Ni(1)-S(1)	88.32(2)
		S(2)-Ni(1)-P(1)	44.89(2)

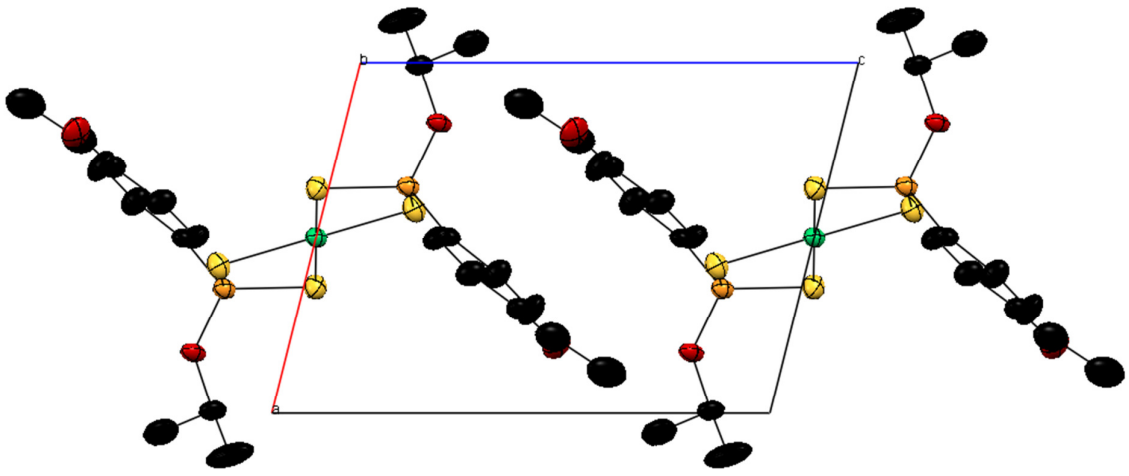

Figure 3.5: Packing diagram of 2A viewed along the b axis. Hydrogen atoms have been omitted for clarity.

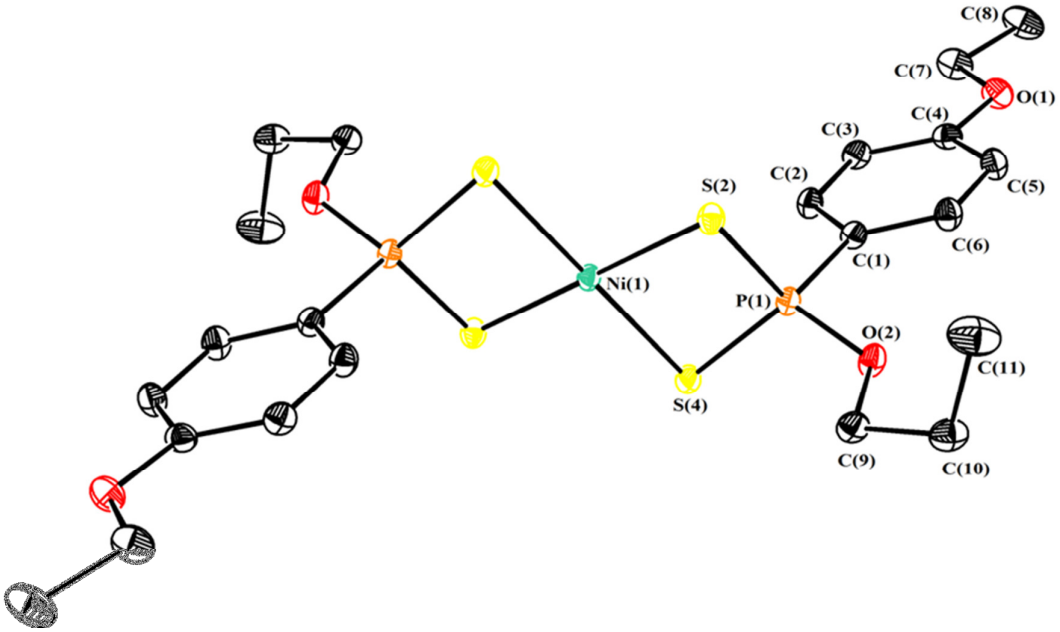

Figure 3.6: Molecular structure of complex 3A. ORTEP diagram, thermal ellipsoids drawn at 50% probability, symmetric ellipsoids were generated by symmetry code 1-x, -y, 1-z and have not been labelled. Hydrogen atoms are omitted for clarity

Table 3.5: Selected bond lengths (Å) and angles (°) for 3A

O(2)-P(1)	1.5822(7)	C(9)-O(2)-P(1)	120.67(6)
P(1)-S(4)^{i}	2.0026(4)	O(2)-P(1)-C(1)	100.55(4)
P(1)-S(2)	2.0081(3)	O(2)-P(1)-S(4)^{i}	114.86(3)
P(1)-Ni(1)	2.8310(3)	C(1)-P(1)-S(4)^{i}	113.69(3)
S(2)-Ni(1)	2.2264(2)	O(2)-P(1)-S(2)	113.25(3)
S(4)-P(1)	2.0026(4)	C(1)-P(1)-S(2)	113.57(3)
S(4)-Ni(1)	2.2254(2)	S(4)-P(1)-S(2)	101.530(15)
		O(2)-P(1)-Ni(1)	139.70(3)
		C(1)-P(1)-Ni(1)	119.74(3)
		S(4)-P(1)-Ni(1)	51.409(9)
		S(2)-P(1)-Ni(1)	51.421(9)
		P(1)-S(2)-Ni(1)	83.742(11)
		P(1)^{i}-S(4)-Ni(1)	83.894(11)
		S(4)-Ni(1)-S(2)^{i}	88.502(9)
		S(4)-Ni(1)-S(2)	91.498(9)

*Symmetry code : (i) 1-x, -y, 1-z

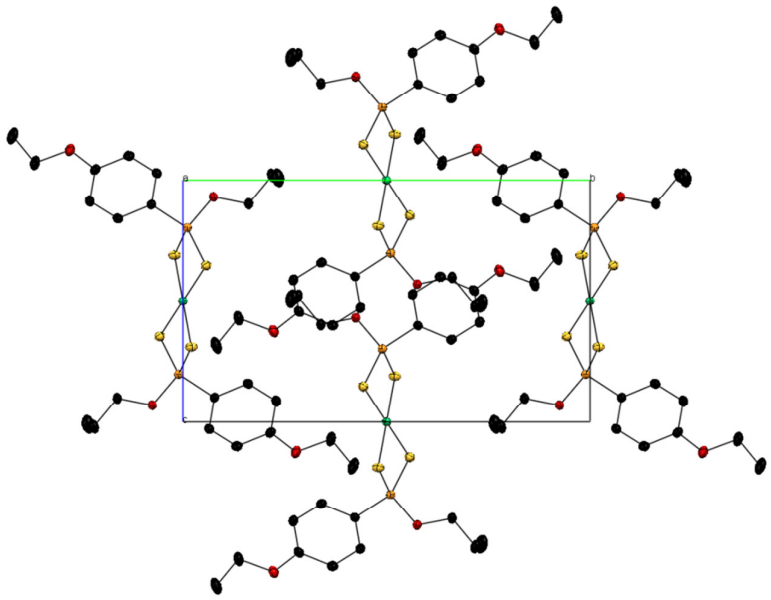

Figure 3.7: Crystallographic packing of complex 3A viewed along the a axis. Hydrogen atoms have been omitted for clarity.

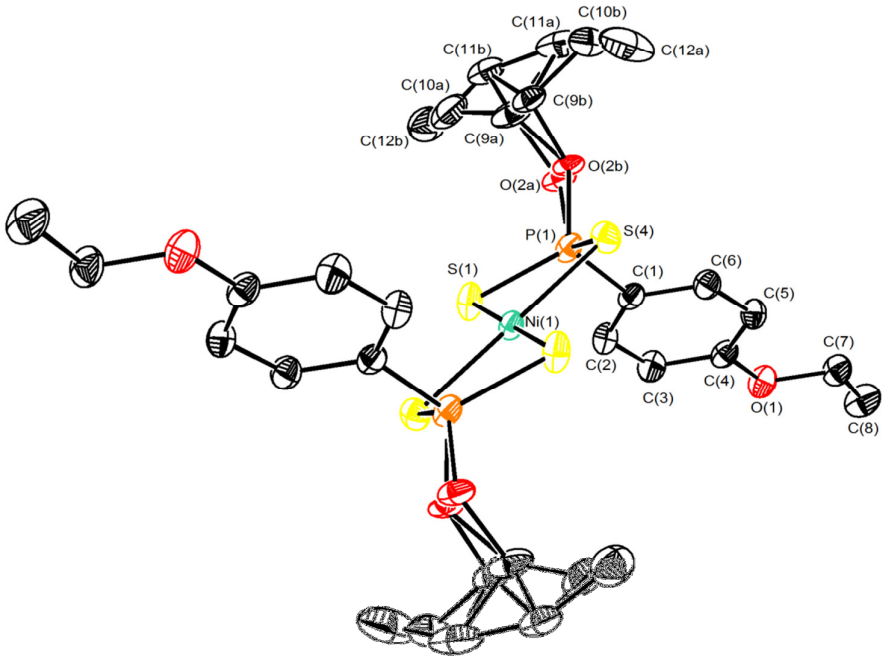

Figure 3.8: Molecular structure of complex 4A. ORTEP diagram, thermal ellipsoids drawn at 50% probability, symmetric ellipsoids were generated by symmetry code -x, 1-y, 1-z and have not been labelled. Hydrogen atoms are omitted for clarity.

Table 3.6: Selected bond lengths (Å) and angles (°) for 4A

Ni(1)-S(4)	2.2256(3)	O(2a)-P(1)-C(1)	99.2(5)
Ni(1)-S(1)	2.2327(3)	O(2b)-P(1)-C(1)	99.6(5)
Ni(1)-P(1)	2.8282(3)	C(1)-P(1)-S(1)	113.60(4)
P(1)-O(2A)	1.490(11)	O(2a)-P(1)-S(4)	118.5(5)
P(1)-O(2B)	1.663(9)	O(2b)-P(1)-S(4)	110.5(4)
P(1)-S(1)	2.0040(5)	C(1)-P(1)-S(4)	113.88(4)
P(1)-S(4)	2.0051(4)	S(1)-P(1)-S(4)	101.483(18)
		O(2a)-P(1)-Ni(1)	141.9(5)
		O(2b)-P(1)-Ni(1)	141.4(5)
		C(1)-P(1)-Ni(1)	118.70(4)
		S(1)-P(1)-Ni(1)	51.672(11)
		S(4)-P(1)-Ni(1)	51.465(11)
		P(1)-S(1)-Ni(1)	83.569(14)
		P(1)-S(4)-Ni(1)	83.729(14)
		C(9A)-O(2A)-P(1)	126.3(10)
		S(4)-Ni(1)-S(1)	88.260(12)

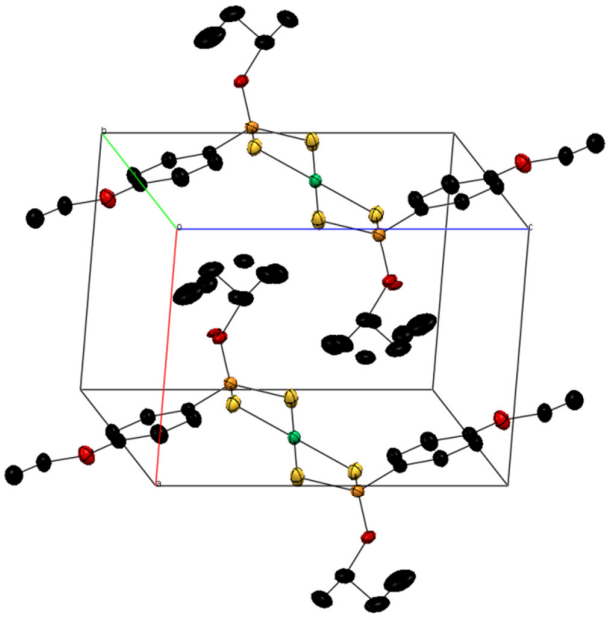

Figure 3.9: Crystallographic packing of complex 4A viewed along the b axis. Hydrogen atoms have been omitted for clarity.

Table 3.7: Crystal data and structure refinement for complexes 1A, 2A, 3A and 4A

Complex	**1A**	**2A**	**3A**	**4A**
Empirical formula	$C_{18}H_{24}NiO_4P_2S_4$	$C_{22}H_{32}NiO_4P_2S_4$	$C_{22}H_{32}NiO_4P_2S_4$	$C_{24}H_{36}NiO_4P_2S_4$
Formula weight	553.26	609.37	609.37	637.42
Temperature	173(2) K	173(2) K	173(2) K	173(2) K
Wavelength	0.71073 Å	0.71073 Å	0.71073 Å	0.71073 Å
Crystal system	Monoclinic	Triclinic	Monoclinic	Triclinic
Space group	P21/c	P-1	P21/c	P-1
Unit cell dimensions	a = 13.5866(5) Å b = 6.4212(2) Å c = 14.1047(5) Å	7.8893(6) 8.4178(7) 11.4825(10)	a = 9.4227(2) Å b = 15.6479(3) Å c = 9.5281(2) Å	a = 7.8787(2) Å b = 9.6995(2) Å c = 10.7728(2) Å
	α= 90° β= 109.389(2)° γ = 90°	α = 109.530(4) ° β = 101.959(4) ° γ = 93.913(5) °	α= 90° β= 102.8780(10)° γ = 90°	α= 103.732(2)° β= 94.723(2)° γ = 106.298(2)°
Volume	1160.74(7) $Å^3$	695.22(10) $Å^3$	1369.54(5) $Å^3$	757.72(3) $Å^3$
Z	2	1	2	1
Density (calculated)	1.583 Mg/m^3	1.456 Mg/m^3	1.478 Mg/m^3	1.397 Mg/m^3
Absorption coefficient	1.356 mm^{-1}	1.139 mm^{-1}	1.157 mm^{-1}	1.049 mm^{-1}
F(000)	572	318	636	334
Crystal size	0.43 x 0.31 x 0.24 mm^3	0.14 x 0.26 x 0.39 mm^3	0.40 x 0.34 x 0.11 mm^3	0.19 x 0.11 x 0.11 mm^3
Theta range for data collection	2.94 to 28.37°	2.6 to 27.5°	2.22 to 28.49°	1.97 to 28.35°
Index ranges	-18<=h<=17, -8<=k<=8, -18<=l<=18	0<=h<=10, -10<=k<=10, -14<=l<=14	-12<=h<=12, -20<=k<=20, -12<=l<=12	-10<=h<=10, -12<=k<=12, -13<=l<=14
Reflections collected	19824	14410	32798	25243
Independent reflections	2850 [R(int) = 0.0362]	3062 [R(int) = 0.0351]	3446 [R(int) = 0.0199]	3770 [R(int) = 0.0281]
Completeness to theta	θ = 28.37° 98.1 %	θ = 27.45° 96.3 %	θ =28.49° 99.5 %	θ = 28.35° 99.40%
Absorption correction	Semi-empirical from equivalents	Semi-empirical from equivalents	Semi-empirical from equivalents	Semi-empirical from equivalents
Max. and min. transmission	0.7367 and 0.5932	0.8586 and 0.6649	0.8833 and 0.6547	0.8934 and 0.8256
Refinement method	Full-matrix least-squares on F^2	Full-matrix least-squares on F^2	Full-matrix least-squares on F^2	Full-matrix least-squares on F^2
Data / restraints / parameters	2850 / 2 / 135	3062 / 0 / 154	3446 / 0 / 153	3770 / 0 / 211
Goodness-of-fit on F^2	1.069	1.021	1.085	1.06
Final R indices [I>2sigma(I)]	R1 = 0.0232, wR2 = 0.0598	R1 = 0.0303, wR2 = 0.0593	R1 = 0.0186, wR2 = 0.0522	R1 = 0.0223, wR2 = 0.0575
R indices (all data)	R1 = 0.0263, wR2 = 0.0623	R1 = 0.0534, wR2 = 0.0654	R1 = 0.0193, wR2 = 0.0529	R1 = 0.0246, wR2 = 0.0593
Largest diff. peak and hole	0.562 and -0.442 $e.Å^{-3}$	0.269 and -0.305 $e.Å^{-3}$	0.350 and -0.387 $e.Å^{-3}$	0.316 and -0.306 $e.Å^{-3}$

3.2.4 An Octahedral Ni(II) Dithiophosphonate complex

Distorted square planar Ni(II) dithiophosphonate complexes have been previously shown to accommodate secondary ligand species, resulting in complexes in which the central Ni atom adopts a higher 6 co-ordination mode.[17] Attempts to synthesize increased co-ordination Ni(II) complexes were made in this study using complexes **1A**, **2A**, **3A** and **4A,** and 4-*tert*butyl pyridine as an auxiliary ligand. All attempts to increase the coordination number around the Ni centre seemed successful as a colour change from purple to green was observed when pyridine to equimolar ratios of the complexes in toluene. An adduct of **4A** was thus formed, **4Ai**, was the only adduct that rendered green crystals for X-ray analysis.

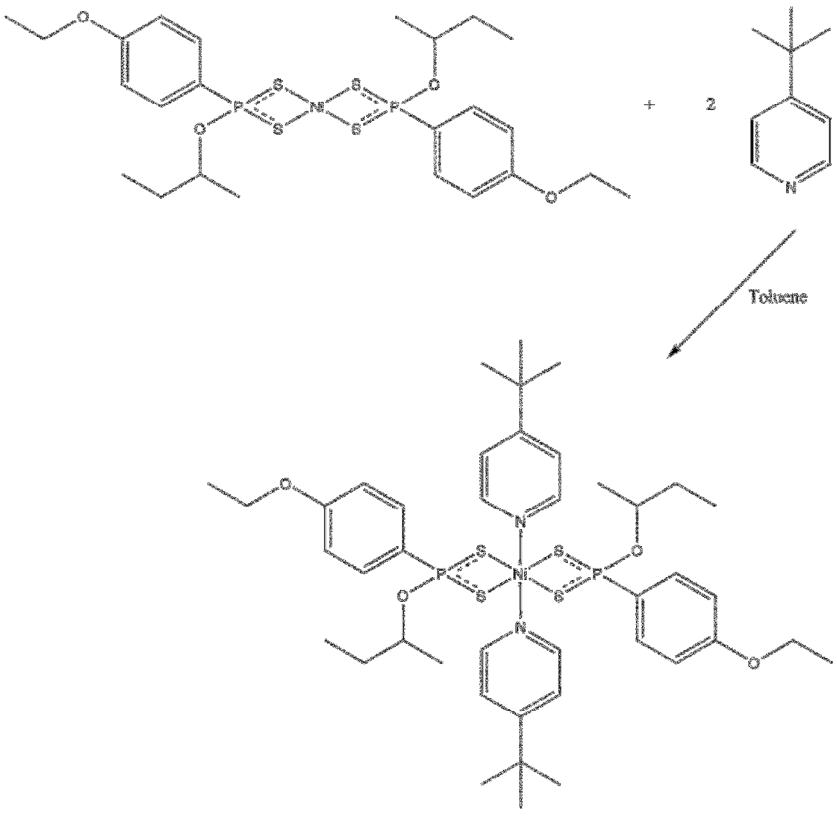

Scheme 3.3: Formation of the octahedral nickel(II) complex, 4Ai

3.2.4.1 Characterization

Characterization of the product was made mainly by infrared spectroscopy. Comparison of spectra of **4A** and **4Ai** showed the appearance of a weak band at the 426 cm^{-1}, to which the Ni-N stretch was assigned since it was absent in **4A**. The melting point of **4Ai** showed an interesting colour change from green to purple at 164 °C, while complete melting occurred at 185 °C. Elemental analysis of **4Ai** was consistent with calculated data (see **Chapter 2**).The formation and solid-state molecular structure of **4Ai** was unambiguously confirmed by X-ray crystallography. NMR studies could unfortunately not be satisfactorily conducted due to the high spin state of the nickel rendering it paramagnetic and thus unsuitable for NMR analysis

3.2.4.2 Crystallographic study

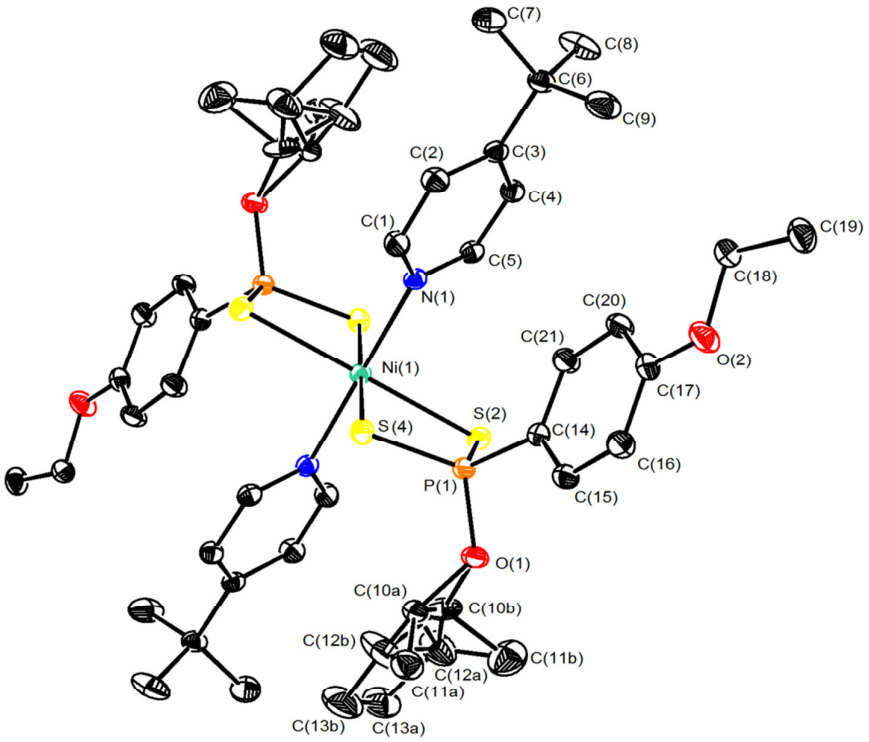

Figure 3.10: Crystal structure of complex 4Ai. ORTEP diagram, thermal ellipsoids drawn at 50% probability, symmetric ellipsoids were generated by symmetry code 2-x, 1-y, 1-z and have not been labelled, Hydrogen atoms are omitted for clarity.

As with the molecular structure of **4A**, **Figure 3.8**, disorder was evident in the alkyl chain of the 2-butoxy group of **4Ai**, **Figure 3.10**, for presumably similar reasons to those discussed above. Unlike **4A**, however, no disorder of the O(1) atom was evident in **4Ai**. This is due to unique intermolecular O··H interactions [2.507(1) Å], with the O atom of one complex molecule interacting with an H atom, belonging to the alkyl chain, of an adjacent molecule, **Figure 3.12**. Examination of the molecular structure of **4Ai** showed that the 4-tert butyl pyridine ligands occupied axial positions perpendicular to the square plane comprising the Ni and S atoms, with N-Ni-S bond angles ranging from 89.71 to 90.82° (**Table 3.8**). The centre of symmetry was thus maintained at the Ni atom, in this regard the structure of **4Ai** is related to that reported by Porta and co-workers in 1971 and by Aragoni and co-workers in 2007.[18, 19] The Ni-N bond length was 2.11 Å, shorter than the two equivalent Ni-S bond lengths of 2.49 Å. Further comparison of bond length data of **4A** (**Table 3.6**) and **4Ai** showed that elongation of Ni-S bonds occurred upon binding of the pyridine-based ligands, and while P-S bond lengths shortened, the two P-S bond lengths in the asymmetric unit of **4Ai** were still equivalent, and thus the isobidentate binding had not changed. The adduct, **4Ai**, belongs to the same triclinic crystal system and belongs to the same cetrosymmetric space group as complex **4A**.[16]

Table 3.8: Selected bond lengths (Å) and angles (°) for 4Ai

N(1)-Ni(1)	2.1100(10)	O(1)-P(1)-C(14)	98.71(6)
O(1)-P(1)	1.5947(10)	O(1)-P(1)-S(2)	113.35(4)
P(1)-S(2)	1.9964(5)	C(14)-P(1)-S(2)	112.69(5)
P(1)-S(1)	2.0008(4)	O(1)-P(1)-S(1)	112.62(4)
S(1)-Ni(1)	2.4931(3)	C(14)-P(1)-S(1)	110.57(4)
S(2)-Ni(1)	2.4919(3)	S(2)-P(1)-S(1)	108.67(2)
		P(1)-S(1)-Ni(1)	84.837(14)
		P(1)-S(2)-Ni(1)	84.959(14)
		N(1)-Ni(1)-N(1)^{i}	180.000(1)
		N(1)-Ni(1)-S(2)	89.71(3)
		N(1)^{i}-Ni(1)-S(2)	90.29(3)
		N(1)-Ni(1)-S(2)^{i}	90.29(3)
		N(1)-Ni(1)-S(1)	90.82(3)
		S(2)-Ni(1)-S(1)	81.300(10)

*Symmetry code : (i) 2-x, 1-y, 1-z

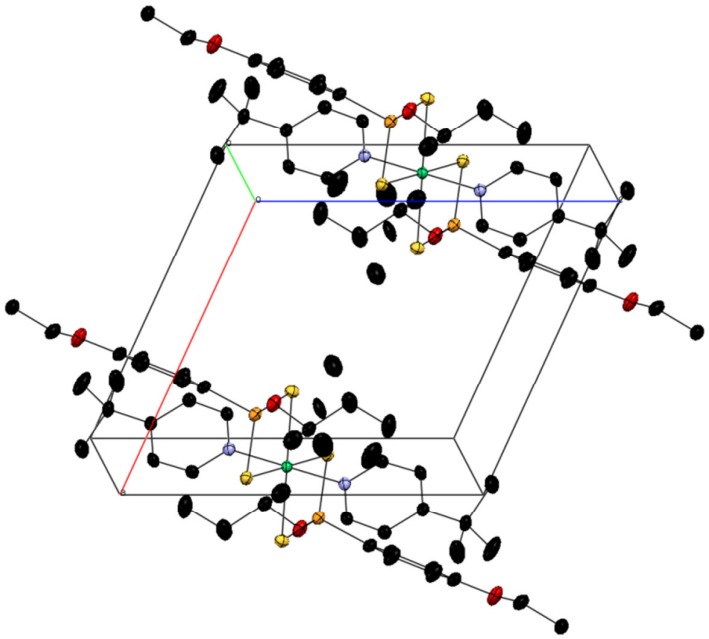

Figure 3.11: Packing of 4Ai viewed along the b axis. Hydrogen atoms are omitted for clarity.

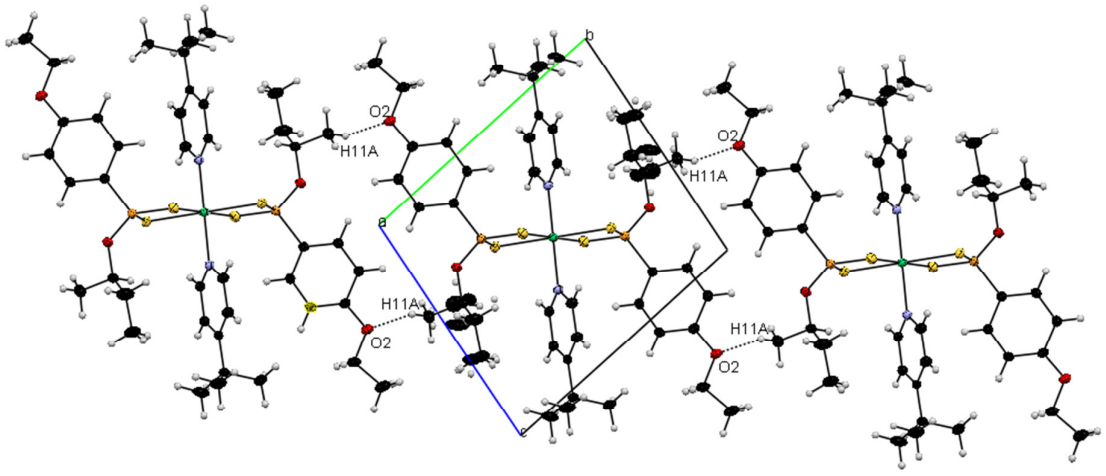

Figure 3.12: Intermolecular O···H interactions present in complex 4Ai viewed along the a axis

Table 3.9: Crystal data and structure refinement for 4Ai

Empirical formula	C_{42} H_{62} N_2 Ni O_4 P_2 S_4
Formula weight	907.83
Temperature	173(2) K
Wavelength	0.71073 Å
Crystal system	Triclinic
Space group	P-1
Unit cell dimensions	a = 9.9917(2) Å b = 11.1913(2) Å c = 11.2033 (2) Å
	α= 94.6560(10)° β= 114.7120(10)° γ = 96.1520(10)°
Volume	1120.41(4) $Å^3$
Z	1
Density (calculated)	1.345 Mg/m3
Absorption coefficient	0.733 mm-1
F(000)	482
Crystal size	0.30 x 0.27 x 0.20 mm3
Theta range for data collection	1.85 to 28.40°.
Index ranges	-13<=h<=13, -14<=k<=14, -14<=l<=14
Reflections collected	34326
Independent reflections	5538 [R(int) = 0.0242]
Completeness to theta	θ = 28.40° 98.50%
Absorption correction	Semi-empirical from equivalents
Max. and min. transmission	0.8673 and 0.8101
Refinement method	Full-matrix least-squares on F2
Data / restraints / parameters	5538 / 0 / 295
Goodness-of-fit on F^2	1.049
Final R indices [I>2sigma(I)]	R1 = 0.0257, wR2 = 0.0644
R indices (all data)	R1 = 0.0291, wR2 = 0.0663
Largest diff. peak and hole	0.446 and -0.292 e.Å-3

In summary: This chapter presented the successful formation of four dithiophosphonate ligands used in this study. It also presented the formation of four new Ni(II) dithiophosphonato complexes and the molecular structures thereof, with crystallographic data of all the complexes contained being fully discussed. The molecular structure of a new octahedral Ni(II) adduct was also discussed. Characterization of the new compounds contained in this chapter was also presented. The new complexes described in this chapter were found to be structurally similar to those previously reported.

3.3 References

1. W. E. Van Zyl and J. P. Fackler, *Phosphorus, Sulfur Silicon Relat. Elem.*, 2000, **167**, 117-132.
2. L. C. Thomas and R. A. Chittenden, *Spectrochimica Acta*, 1964, **20**, 489-502.
3. J. Coates, in *Encyclopedia of Analytical Chemistry*, John Wiley & Sons, Ltd, 2006.
4. L. Malatesta and R. Pizzotti, *Gazz. Chim. Ital.*, 1946, **76**, 167.
5. H. Hartung, *Z. Chem.*, 1967, **7**, 241-241.
6. I. P. Gray, A. M. Z. Slawin and J. D. Woollins, *Dalton Trans.*, 2004, 2477-2486.
7. Y. Ozcan, S. Ide, M. Karaku and H. Yilmaz, *Anal. Sci.*, 2002, **18**, 1285-1286.
8. M. Arca, A. Cornia, F. A. Devillanova, A. C. Fabretti, F. Isaia, V. Lippolis and G. Verani, *Inorg. Chim. Acta*, 1997, **262**, 81-84.
9. M. C. Aragoni, M. Arca, F. A. Devillanova, M. B. Hursthouse, S. L. Huth, F. Isaia, V. Lippolis, A. Mancini, S. Soddu and G. Verani, *Dalton Trans.*, 2007, 2127-2134.
10. S. Sewpersad, B. Omondi and W. E. Van Zyl, *Acta Crystallogr., Sect. E: Struct.*, 2012, **68**, m1483.
11. S. Sewpersad and W. E. Van Zyl, *Acta Crystallogr., Sect. E: Struct.*, 2012, **68**, m1457.
12. S. Sewpersad, B. Omondi and W. E. Van Zyl, *Acta Crystallogr., Sect. E: Struct.*, 2012, **68**, m1534.
13. W. E. Van Zyl, *Comments Inorg. Chem.*, 2010, **31**, 13-45.
14. J. E. Huheey, E. A. Keiter and R. L. Keiter, *Inorganic Chemistry Principles of Structure and Reactivity*, Fourth edn., Harper Collins College Publishers, 1993.
15. I. Haiduc, D. B. Sowerby and S.-F. Lu, *Polyhedron*, 1995, **14**, 3389-3472.
16. H. Burzlaff and H. Zimmerman, International Union of Crystallography, 2006, vol. Volume A: Space Group Symmetry, pp. 818 - 820.

17. M. C. Aragoni, M. Arca, M. Crespo, F. A. Devillanova, M. B. Hursthouse, S. L. Huth, F. Isaia, V. Lippolis and G. Verani, *Dalton Trans.*, 2009, 2510-2520.

18. M. C. Aragoni, M. Arca, M. Crespo, F. A. Devillanova, M. B. Hursthouse, S. L. Huth, F. Isaia, V. Lippolis and G. Verani, *CrystEngComm*, 2007, **9**, 873-878.

19. P. Porta, A. Sgamellotti and N. Vinciguerra, *Inorg. Chem.*, 1971, **10**, 541-547.

Chapter 4: Dithiophosphonate Complexes of the Group 12 Metals Cadmium and Mercury

Dithiophosphonate complexes of all group 12 metals have been previously reported.[1-5] Three new group 12 metal dithiophosphonate complexes have been synthesized and characterized in the present study, two mercury(II) complexes, **1B** and **2B**[6] and one cadmium(II) complex, **1C**.

4.1 Complex preparation

Complexes **1B**, **2B** and **1C** were all produced by similar methods. Four stoichiometric equivalents of the respective dithiophosphonate salt (**1** and **2**) were dissolved in methanol, while two stoichiometric equivalents of the respective metal salt either $Cd(NO_3)_2 \cdot 4H_2O$ or $Hg(NO_3)_2 \cdot H_2O$ were dissolved in water, forming clear solutions in both cases. Addition of the respective metal ion solutions to the respective ligands resulted in immediate white precipitation in all three cases which indicated the formation of the expected complexes following work-up. The solid products were readily isolated by filtration as the ammonium nitrate by-product was soluble in the aqueous reaction media. All crystals were colourless and grown by slow diffusion of hexane into a DCM solution of the respective complex.

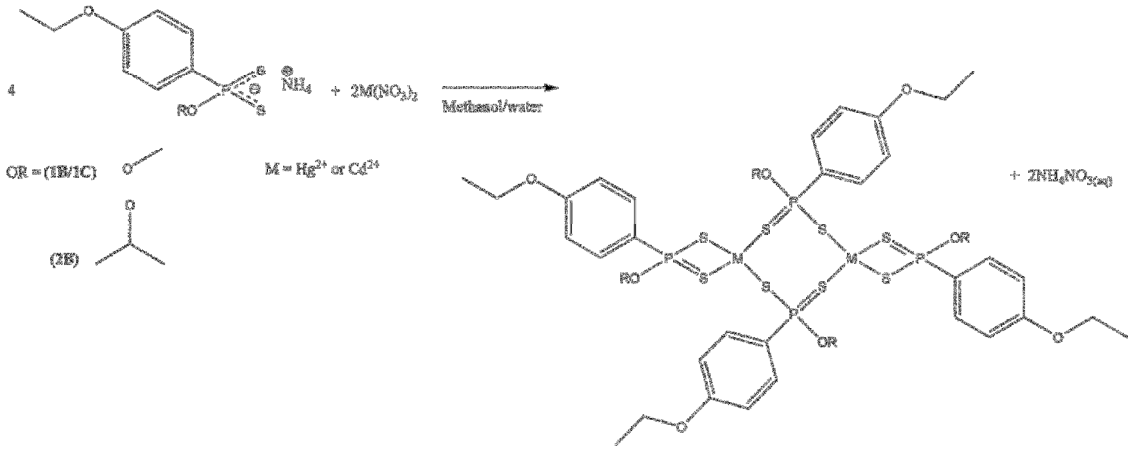

Scheme 4.1: Formation of Group 12 dithiophosphonato complexes

4.2 Characterization

Yields of the synthesized group 12 metal complexes bearing ligand **1** (**Table 4.1**) were generally low and comparable to that of the related nickel complex (**Table 3.2**). In the case of **2B**, however, the yield of the mercury complex was significantly lower than the nickel counterpart (**2A**). This was due to a difference in nuclearity between the two complexes giving rise to more equilibrium reactions, stemming from the preference of the ligand to adopt resonance structure **L** over **J/K** (**Figure 1.3**) in this type of complex.

Table 4.1: Characterization data of Group 12 metal complexes

Complex	Ligand Alkoxy Group	Metal Cation	Melting point / °C	Yield / %	^{31}P NMR shift / ppm
1B	Methoxy	Hg^{2+}	120 (decomp)	31	106
1C	Methoxy	Cd^{2+}	157 - 158	47	109
2B	2-propoxy	Hg^{2+}	117 - 118	43	101

All of the group 12 metal dithiophosphonate complexes had sharp melting point ranges indicating high relative purity of the bulk products. The melting point temperatures of the respective group 12 complexes were found to be lower than those of the analogous Ni(II) complexes reported in this study.[7] Elemental analyses of the group 12 complexes was consistent with calculated data (see **Chapter 2**). Infrared spectra of the complexes were consistent with data previously discussed for the ligand IR assignment (**3.1.2**), and as with the Ni(II) complexes disappearance of the broad N-H stretching bands were indicative of complex formation.

The group 12 dithiophosphonate complexes were subjected to solution NMR examination (^{1}H, ^{31}P and ^{13}C) in $CDCl_3$. The ^{1}H and ^{13}C NMR spectra confirmed the presence of the phenetyl and respective alkoxy groups. The ^{31}P spectrum of each of the complexes showed sharp singlets, indicating presence of all P atoms in chemically equivalent positions. As for the Ni(II) complexes: the ^{31}P singlet peaks of the group 12 complexes appeared further upfield than the free ligand salts.

4.3 Crystallographic studies

Examinations of the crystal structures of **1B**, **2B** and **1C** (**Figures 4.1, 4.4** and **4.6** respectively) revealed that they are quite similar to structures previously reported *i.e.* dinuclear, neutral, and 4-coordinate around each metal centre.[1] The S-M-S bond angles for each of the complexes reported varied widely **1B** 78.59 - 141.29° , **2B** 76.26 - 154.65°, **1C** 79.40 – 129.59° illustrating the distorted tetrahedron arrangement around the metal atoms. The dinuclear group 12 complexes in this study each comprise four ligand molecules, two of which chelate the metal centres, while the other two form bridges between them. An eight-membered metallo-ring comprising the metal, sulfur and phosphorus atoms is formed. The ligands bind the metals in an anisobidentate manner as was evident from the two longer M-S

bonds (**1B:** 2.7514 Å, 2.6947 Å, **2B:** 2.9361 Å, 2.8105 Å, **1C:** 2.6394 Å, 2.5811 Å) and two shorter M-S bonds (**1B:** 2.4752 Å, 2.4216 Å, **2B:** 2.4042 Å, 2.3997 Å, **1C:** 2.5262 Å, 2.4966 Å), one of each belonging to a separate ligand unit (a bridging- and chelating ligand). The result of this pattern was the formation of an inversion centre within the complex, between the two metal atoms. Complexes **1B** and **1C** were both shown to hold similar groups of ligands adjacent to one another within the complex molecule *i.e.* the phenetole groups of a bridging and chelating ligand were held adjacent to one another, while in the case of **2B,** the groups of a single molecule were arranged in an alternating pattern with a phenetole group flanked by two alkyl chains and *vice versa*. The formation of this alternating pattern was presumably due the increased length of the alkoxy group, and the resultant geometry can thus be ascribed to steric reasons.

In **Figures 4.2** and **4.6** the crystallographic packing of complexes **1B** and **1C** are illustrated, both are monoclinic and belong to space group P21/c, thereby indicating that they are centrosymmetric.[8] **Figure 4.4** shows the crystallographic packing of complex **2B**, similar to the analagous nickel(II) (**2A**) and lead(II) (**2D**) complexes, it also crystallizes in a triclinic crystal system and belongs to the centrosymmetric space group P-1. [8] Inspection of **Table 4.5** revealed that complex **1B** was found to have the greatest density of the group 12 complexes, greater than both its Cd(II) analogue (**1C**) and complex **2B**, which bears the similar Hg(II) nuclei. Thus it can be stated that **1B** had the most efficient crystal packing of the group 12 dithiophosphonate complexes. The methoxy complexes **1B** and **1C** were both found to have significantly greater unit cell volumes than the 2-propoxy complex **2B**, as demonstrated in section **3.2.3**, the lower unit cell volume of **2B** was due to the secondary nature of the alkoxy substituent in the ligands.

Complex **1B** contains intermolecular O···S interactions as shown in **Figure 4.2**. One complex interacts with four neighbouring complexes through both the alkoxy O atoms and two bridging S atoms, each belonging to a separate bridging unit, the M···O distance for this interaction was found to be 3.320(2) Å. It is also evident from **Figure 4.2** that this interaction may be of sufficient energy to direct the packing forces of the crystal lattice.

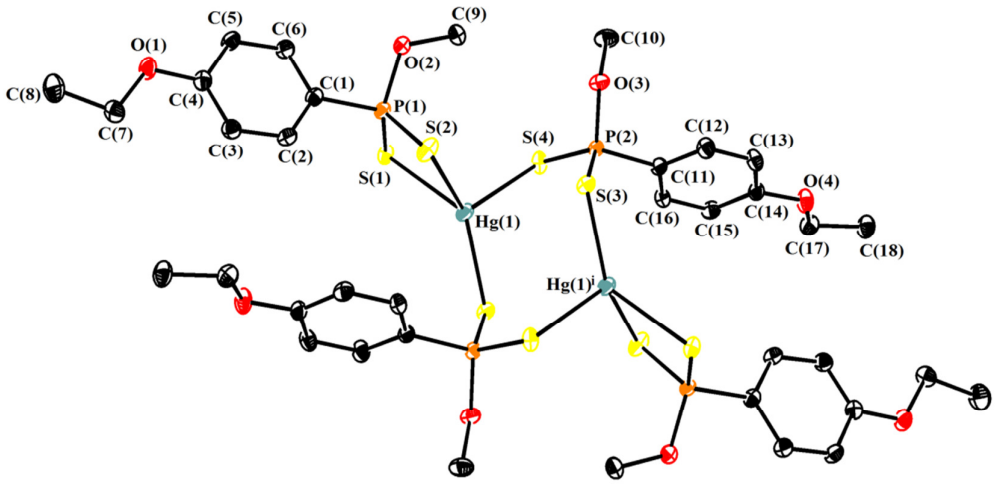

Figure 4.1: Molecular structure of complex 1B. ORTEP diagram, thermal ellipsoids drawn at 50% probability, symmetric ellipsoids were generated by symmetry code 1-x, 2-y, -z and have not been labelled. Hydrogen atoms are omitted for clarity.

Table 4.2: Selected bond lengths (Å) and angles (°) for 1B

O(2)-P(1)	1.598(2)	C(1)-P(1)-S(1)	113.37(11)
P(1)-S(1)	1.9901(12)	O(2)-P(1)-S(2)	109.80(10)
P(1)-S(2)	2.0343(12)	C(1)-P(1)-S(2)	110.36(12)
S(1)-Hg(1)	2.7514(9)	S(1)-P(1)-S(2)	111.01(5)
S(2)-Hg(1)	2.4752(10)	P(1)-S(1)-Hg(1)	81.17(4)
S(3)-Hg(1)^{i}	2.4216(9)	P(1)-S(2)-Hg(1)	87.63(4)
S(4)-Hg(1)	2.6947(9)	P(2)-S(3)-Hg(1)^{i}	99.70(4)
P(2)-S(4)	1.9882(12)	S(3)^{i}-Hg(1)-S(2)	141.29(3)
P(2)-S(3)	2.0424(12)	S(3)^{i}-Hg(1)-S(4)	97.76(3)
P(2)-C(11)	1.795(3)	S(2)-Hg(1)-S(4)	115.31(3)
C(1)-P(1)	1.795(3)	S(3)^{i}-Hg(1)-S(1)	121.55(3)
O(3)-P(2)	1.603(2)	S(2)-Hg(1)-S(1)	78.59(3)
		S(4)-Hg(1)-S(1)	92.22(3)
		O(2)-P(1)-S(1)	112.23(11)
		O(2)-P(1)-C(1)	99.54(14)
		P(2)-S(4)-Hg(1)	99.37(4)
		O(3)-P(2)-S(3)	98.02(10)
		C(11)-P(2)-S(4)	109.71(12)
		O(3)-P(2)-S(4)	112.62(10)
		O(3)-P(2)-C(11)	106.87(14)
		C(11)-P(2)-S(3)	111.82(11)

*Symmetry code : (i) 1-x, 2-y, -z

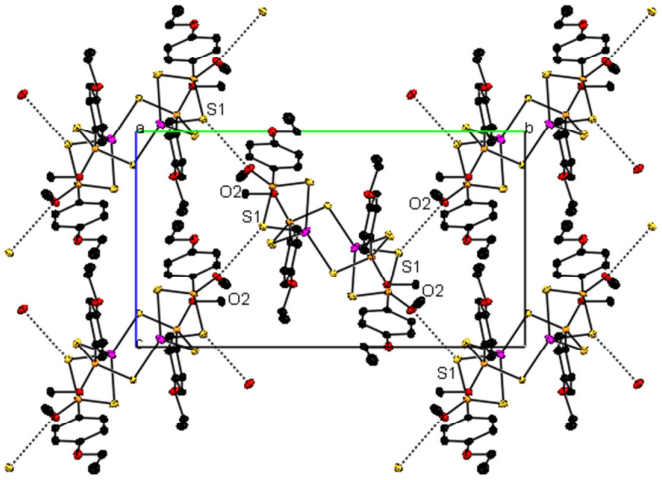

Figure 4.2: A portion of the packing in the crystal structure of complex 1B viewed along the a axis showing intermolecular S···O interactions. Hydrogen atoms have been omitted for clarity.

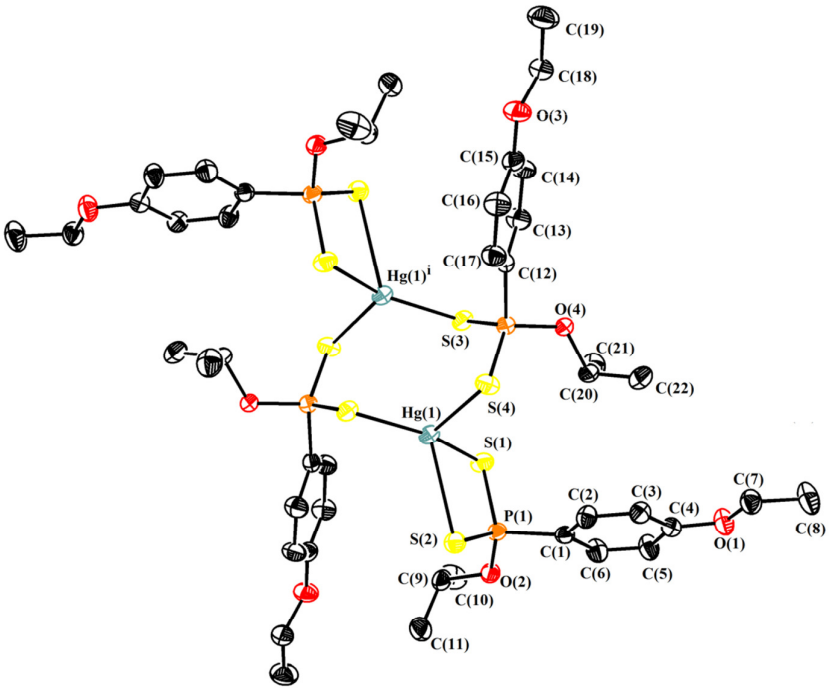

Figure 4.3: Molecular structure of complex 2B. ORTEP diagram, thermal ellipsoids drawn at 50% probability, symmetric ellipsoids were generated by symmetry code 1-x, 2-y, -z and have not been labelled, hydrogen atoms are omitted for clarity.

Table 4.3: Selected bond lengths (Å) and angles (°) for 2B

Hg(1) -S(1)	2.4042(10)	S(1)-Hg(1)-S(2)	76.26(2)
Hg(1)-S(2)	2.9361(11)	S(1)-Hg(1)-S(4)	112.32(2)
Hg(1)-S(4)	2.8105(11	S(1)-Hg(1)-S(3)^{i}	154.65(3)
Hg(1)^{i} -S(3)	2.3997(10)	S(2)-Hg(1)-S(4)	97.22(2)
S(1)-P(1)	2.0519(13)	S(2)-Hg(1)-S(3)^{i}	109.11(2)
S(2)-P(1)	1.9680(11)	S(3)^{i}-Hg(1)-S(4)	91.92(2)
S(3)-P(2)	2.0567(13)	Hg(1)-S(1)-P(1)	92.17(3)
S(4)-P(2)	1.9700(12)	Hg(1)-S(2)-P(1)	79.38(3)
P(1)-O(2)	1.5808(18)	Hg(1)^{i}-S(3)-P(2)	97.48(3)
P(1)-C(1)	1.789(3)	Hg(1)-S(4)-P(2)	94.61(4)
P(2)-O(4)	1.585(2)	S(1)-P(1)-S(2)	111.54(5)
P(2)-C(12)	1.791(2)	S(1)-P(1)-O(2)	107.71(9)
		S(1)-P(1)-C(1)	106.96(8)
		S(2)-P(1)-O(2)	114.83(8)
		S(2)-P(1)-C(1)	114.38(9)
		O(2)-P(1)-C(1)	100.57(11)
		S(3)-P(2)-S(4)	114.55(4)
		S(3)-P(2)-O(4)	104.78(8)
		S(3)-P(2)-C(12)	108.57(13)
		S(4)-P(2)-O(4)	113.62(9)
		S(4)-P(2)-C(12)	113.58(9)
		O(4)-P(2)-C(12)	100.49(11)
		P(1)-O(2)-C(9)	120.42(16)

*Symmetry code : (i) 1-x, 2-y, -z

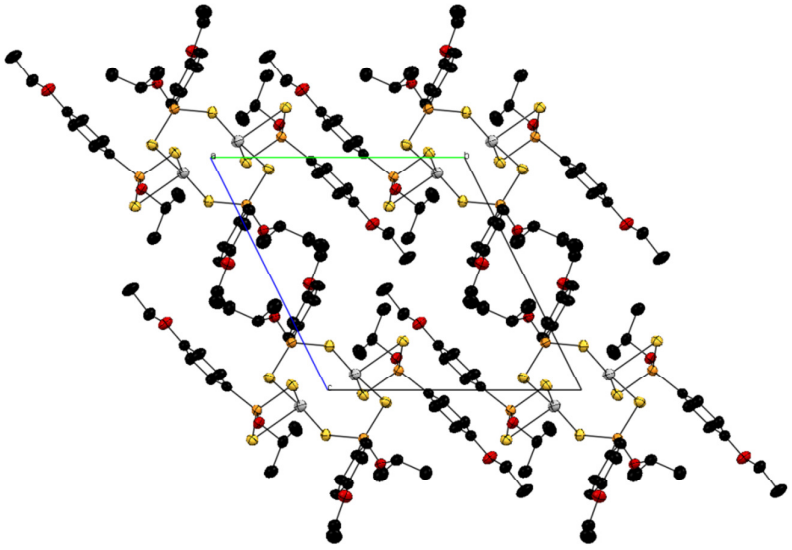

Figure 4.4: Packing of complex 2B viewed along the a axis. Hydrogen atoms are omitted for clarity.

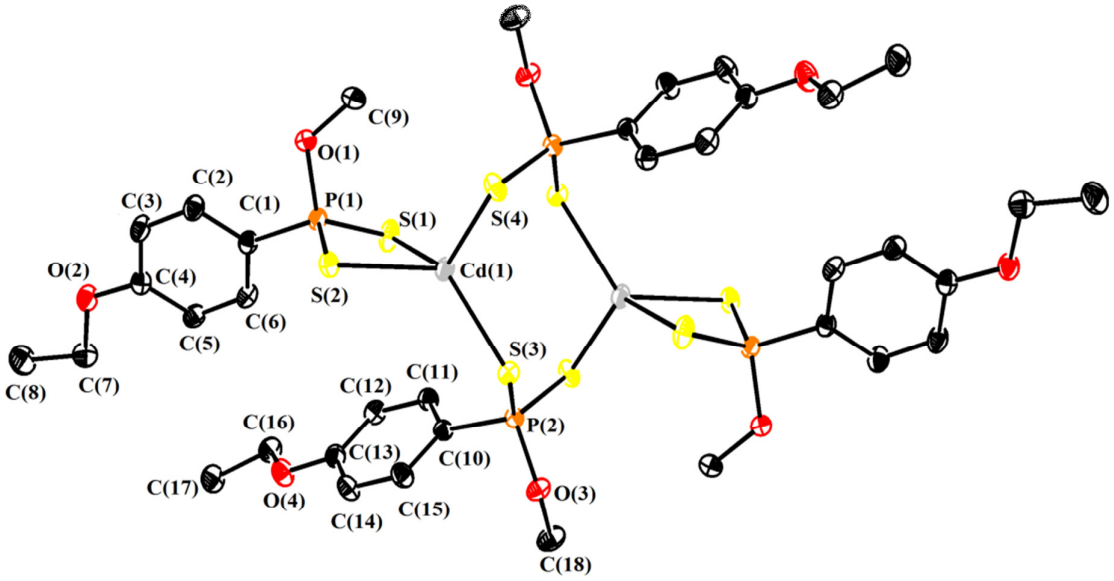

Figure 4.5: Molecular structure of complex 1C. ORTEP diagram, thermal ellipsoids drawn at 50% probability, symmetric ellipsoids were generated by symmetry code 2-x, -y, 2-z and have not been labelled, hydrogen atoms are omitted for clarity.

Table 4.4: Selected bond lengths (Å) and angles (°) for 1C

O(1)-P(1)	1.5962(10)	O(1)-P(1)-C(1)	99.42(5)
O(3)-P(2)	1.5948(9)	C(1)-P(1)-S(2)	112.71(4)
P(1)-S(2)	1.9946(4)	C(1)-P(1)-S(1)	111.55(4)
P(1)-S(1)	2.0121(4)	S(2)-P(1)-S(1)	110.925(19)
P(1)-Cd(1)	3.0717(3)	O(1)-P(1)-Cd(1)	115.11(4)
P(2)-S(4)^{i}	1.9938(4)	C(1)-P(1)-Cd(1)	145.36(4)
P(2)-S(3)	2.0184(4)	O(3)-P(2)-C(10)	106.39(5)
S(1)-Cd(1)	2.5262(3)	C(10)-P(2)-S(4)^{i}	109.29(4)
S(2)-Cd(1)	2.6394(3)	C(10)-P(2)-S(3)	113.97(4)
S(3)-Cd(1)	2.4966(3)	S(4)^{i}-P(2)-S(3)	115.049(19)
S(4)-Cd(1)	2.5811(3)	P(1)-S(1)-Cd(1)	84.384(14)
C(10)-P(2)	1.7870(12)	P(1)-S(2)-Cd(1)	81.757(13)
		P(2)-S(3)-Cd(1)	105.292(15)
		P(2)^{i}-S(4)-Cd(1)	94.855(15)
		S(3)-Cd(1)-S(1)	129.587(12)
		S(3)-Cd(1)-S(4)	98.580(11)
		S(1)-Cd(1)-S(4)	126.796(12)
		S(3)-Cd(1)-S(2)	118.768(10)
		S(1)-Cd(1)-S(2)	79.397(10)
		S(4)-Cd(1)-S(2)	97.862(10)

*Symmetry code : (i) 2-x, -y, 2-z

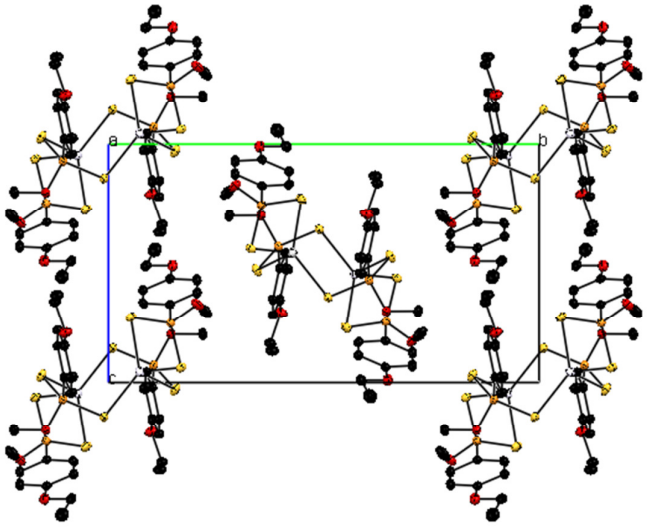

Figure 4.6: Packing of complex 1C viewed along the a axis. Hydrogen atoms have been omitted for clarity.

Table 4.5: Crystal data and structure refinement for complexes 1B, 2B and 1C

Identification code	**1B**	**2B**	**1C**
Empirical formula	C_{36} H_{48} Hg_2 O_8 P_4 S_8	C_{44} H_{64} Hg_2 O_8 P_4 S_8	C_{36} H_{48} Cd_2 O_8 P_4 S_8
Formula weight	1390.28	1502.57	1213.90
Temperature	173(2) K	173(2) K	173(2) K
Wavelength	0.71073 Å	0.71073 Å	0.71073 Å
Crystal system	Monoclinic	Triclinic	Monoclinic
Space group	P21/c	P-1	P21/c
Unit cell dimensions	a = 12.313(3) Å b = 18.892(4) Å c = 10.556(3) Å	a = 11.079(3) Å b = 11.985(3) Å c = 12.253(3) Å	a = 12.3121(2) Å b = 18.8523(3) Å c = 10.5126(2) Å
	α= 90° β= 97.829(9)° γ = 90°	α =62.908(4)° β =84.418(4)° γ =80.862(4)°	α= 90° β= 97.5340(10)° γ = 90°
Volume	2432.7(10) $Å^3$	1429.5(6) $Å^3$	2419.03(7) $Å^3$
Z	2	1	2
Density (calculated)	1.898 Mg/m^3	1.745 Mg/m^3	1.667 Mg/m^3
Absorption coefficient	6.824 mm^{-1}	5.813 mm^{-1}	1.402 mm^{-1}
F(000)	1352	740	1224
Crystal size	0.45 x 0.35 x 0.16 mm^3	0.12 x 0.15 x 0.15 mm^3	0.39 x 0.29 x 0.19 mm^3
Theta range for data collection	1.99 to 25.00°	1.9 to 27.4°	1.99 to 28.29°
Index ranges	-14<=h<=14, -22<=k<=22, -12<=l<=12	-14<=h<=14, -15<=k<=15, -15<=l<=15	-16<=h<=16, -22<=k<=25, -14<=l<=14
Reflections collected	29308	34157	71076
Independent reflections	4199 [R(int) = 0.0374]	6382 [R(int) = 0.0767]	5991 [R(int) = 0.0189]
Completeness to theta	θ = 25.00° 97.8 %	θ = 27.35° 98.6 %	θ = 28.29° 99.9 %
Absorption correction	Semi-empirical from equivalents	Semi-empirical from equivalents	Semi-empirical from equivalents
Max. and min. transmission	0.4081 and 0.1492	0.5422and 0.4759	0.7765 and 0.6108
Refinement method	Full-matrix least-squares on F^2	Full-matrix least-squares on F^2	Full-matrix least-squares on F^2
Data / restraints / parameters	4199 / 2 / 266	6382 / 0 / 304	5991 / 0 / 266
Goodness-of-fit on F^2	1.079	0.965	1.072
Final R indices [I>2sigma(I)]	R1 = 0.0195, wR2 = 0.0504	R1 = 0.0227, wR2 = 0.0465	R1 = 0.0158, wR2 = 0.0390
R indices (all data)	R1 = 0.0212, wR2 = 0.0519	R1 = 0.0294, wR2 = 0.0487	R1 = 0.0177, wR2 = 0.0405
Largest diff. peak and hole	1.402 and -1.017 e.$Å^{-3}$	0.866 and -1.024 e.$Å^{-3}$	0.539 and -0.274 e.$Å^{-3}$

In summary: This chapter addressed the formation and characterization of three new group 12 metal dithiophosphonato complexes, two mercury(II) complexes and one cadmium(II) complex. The crystallographic data of all three complexes contained within this chapter was fully discussed. The new complexes described in this chapter were found to be structurally similar to those previously reported, with no major departures in complex geometry being noted.

4.4 References

1. I. P. Gray, A. M. Z. Slawin and J. D. Woollins, *Dalton Trans.*, 2004, 2477-2486.
2. M. Karakus, H. Yilmaz, Y. Ozcan and S. Ide, *Appl. Organomet. Chem.*, 2004, **18**, 141-142.
3. M. Karakus, H. Yilmaz, E. Bulak and P. Lönnecke, *Appl. Organomet. Chem.*, 2005, **19**, 396-397.
4. W. Shi, M. Shafaei-Fallah, C. E. Anson and A. Rothenberger, *Dalton Trans.*, 2006, 3257-3262.
5. S. Blaurock, F. T. Edelmann, I. Haiduc, G. Mezei and P. Poremba, *Inorg. Chim. Acta*, 2008, **361**, 407-410.
6. S. Sewpersad and W. E. Van Zyl, *Acta Crystallogr., Sect. E: Struct.*, 2012, **68**, m1488-m1489.
7. J. E. Huheey, E. A. Keiter and R. L. Keiter, *Inorganic Chemistry Principles of Structure and Reactivity*, Fourth edn., Harper Collins College Publishers, 1993.
8. H. Burzlaff and H. Zimmerman, International Union of Crystallography, 2006, vol. Volume A: Space Group Symmetry, pp. 818 - 820.

Chapter 5: A Lead(II) Complex

Lead(II) dithiophosphonate complexes are structurally distinctly different to the group 12 and group 10 metal complexes. The Pb(II) complexes have a different type of co-ordination mode giving rise to a variety of crystallographic motifs.[1, 2] Infinite polymeric chains and dimeric pairs, comprising distorted 4-co-ordinate square pyramidal lead(II) units held together by intermolecular Pb···S interactions have been reported for Pb(II) dithiophosphonate complexes. One new neutral Pb(II) dithiophosphonate complex was successfully synthesized and its crystal structure reported in the present study.

5.1 Complex formation

Complex **2D**[3] was produced by addition of an aqueous colourless $Pb(NO_3)_2$ solution to a methanolic solution containing two stoichiometric equivalents of the ammonium dithiophosphonate salt, **2**. This resulted in the immediate formation of an off-white precipitate which was isolated by vacuum filtration, the ammonium nitrate by-product remained in the filtrate due to its solubility in aqueous media.

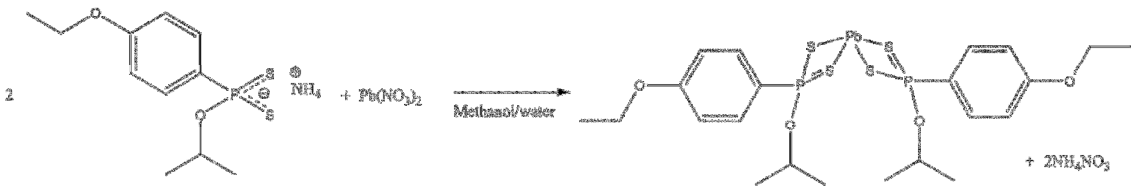

Scheme 5.1: Formation of complex 2D

5.2 General characterization

A quantitative yield of 71% was achieved for complex **2D**, not dissimilar to the high yield found for the related Ni(II) complex containing this ligand, complex **2A** (75% yield).

Complex **2D** was isolated in a significantly higher yield than the analogous dinuclear Hg(II) complex, **2B** (43%). Complex **2D** has a sharp melting point of 130 °C, indicating bulk product purity. The IR spectrum of **2D** was consistent with data previously discussed for the ligand IR assignment (**3.1.1**), pertaining to bands associated with the ligand. The broad N-H stretching bands associated with the ammonium dithiophosphonate salt had disappeared implying complex formation. The solution NMR (^{1}H, ^{31}P and ^{13}C) of **2D** was conducted in $CDCl_3$, and unlike the respective parent dithiophosphonate salt (**2**), the complex was readily soluble in chlorinated solvents. The ^{1}H and ^{13}C NMR spectra confirmed the presence of the phenetyl and 2-propoxy groups. The ^{31}P NMR spectrum of the Pb(II) dithiophosphonate complex showed a sharp singlet at 94 ppm, indicating that the P atoms were chemically equivalent. The shift for the product complex was more upfield than the parent free ligand at 104 ppm. Elemental analysis of **2D** was consistent with calculated data (see **Chapter 2**).

5.3 Crystallographic study

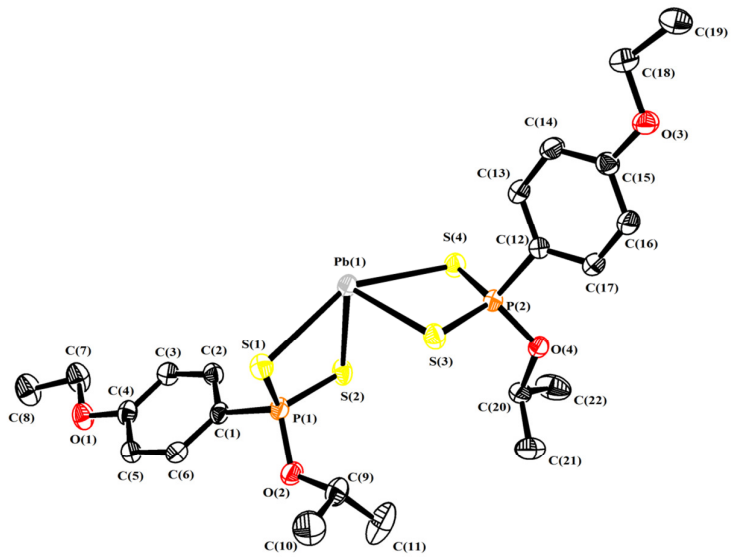

Figure 5.1: Distorted pyramidal molecular structure of complex 2D. ORTEP diagram, thermal ellipsoids drawn at 50% probability. Hydrogen atoms are omitted for clarity.

The crystallographic study confirmed that complex **2D** is a neutral, 4-coordinate, mononuclear complex with a distorted square pyramidal geometry. The apical Pb atom of each pyramid is held at 1.3059(3) Å above the basal S_4 plane and the ligands are anisobidentate. The pyramid is comprised of four Pb-S bonds which varied in length at 2.6999(7), 2.7128(6), 2.8877(7), and 2.9472 (7) Å, clearly showing the presence of two short and two longer bonds. The metal atom is surrounded by two chelating dithiophosphonato ligands binding through the S donor atoms. The P-S bond lengths are also paired as shorter (1.9959 (9), 1.9877 (8) Å) and slightly longer (2.0115 (9), 2.0245 (9) Å), illustrating the anisobidentate nature of the ligand whereby the shorter P-S bond has more double bond character. The S-Pb-S (chelating) bond angles range from 71.841 (18) to 72.692 (19)°, whilst the Pb-S-P bond angles range from 84.70 (3) to 90.51 (3)°

Table 5.1 Selected bond lengths (Å) and angles (°) of 2D

Pb1-S1	2.8877(7)	S1-Pb1-S2	72.69(2)
Pb1-S2	2.6999(7)	S1-Pb1-S3	91.52(2)
Pb1-S3	2.7128(7)	S1-Pb1-S4	149.57(2)
Pb1-S4	2.9472(7)	S2-Pb1-S3	93.09(2)
Pb1-P1	3.3712(7)	S2-Pb1-S4	82.71(2)
Pb1-P2	3.3993(7)	S3-Pb1-S4	71.84(2)
S1-P1	1.9958(9)	P1-Pb1-P2	113.62(1)
S2-P1	2.0114(10)	S3-P2-S4	111.98(4)
S3-P2	2.0245(10)	S1-P1-S2	111.63(4)
S4-P2	1.9878(9)	O2-P1-C1	100.89(10)
P1-O2	1.5876(17)	Pb1-P2-O4	137.11(7)
P1-C1	1.794(2)	Pb1-P2-C12	121.14(8)
P2-O4	1.5848(17)		
P2-C12	1.797(3)		

The crystal structure of complex **2D** is built up of distorted square pyramids in dimeric pairs, **Figure 5.2**. The dimeric pairs showed intermolecular interactions between the Pb atom of one monomer with a S atom of adjacent unit, with a Pb···S distance of 3.6189(7) Å. Similar intermolecular interactions occur between the Pb atom of one unit and four carbon atoms in an aromatic ring of an adjacent unit, Pb···Ar (Ar = aromatic ring) interaction distance range of 3.421-3.597 Å. A related structure with a different alkoxy group was previously reported,[1] showing similar intermolecular Pb···S and Pb···Ar interactions. It was postulated that the aforementioned Pb···Ar interactions stabilized the dimeric structure. The structure reported by Woollins and co-workers adopts a similar molecular unit, the lead atom also resides in the centre of a distorted pyramid, 1.30 Å above the basal S_4 plane.[1] The assymetric unit of complex **2D** belongs to the triclinic system in centrosymmetric space group P-1, **Figure 5.3**.[4, 5]

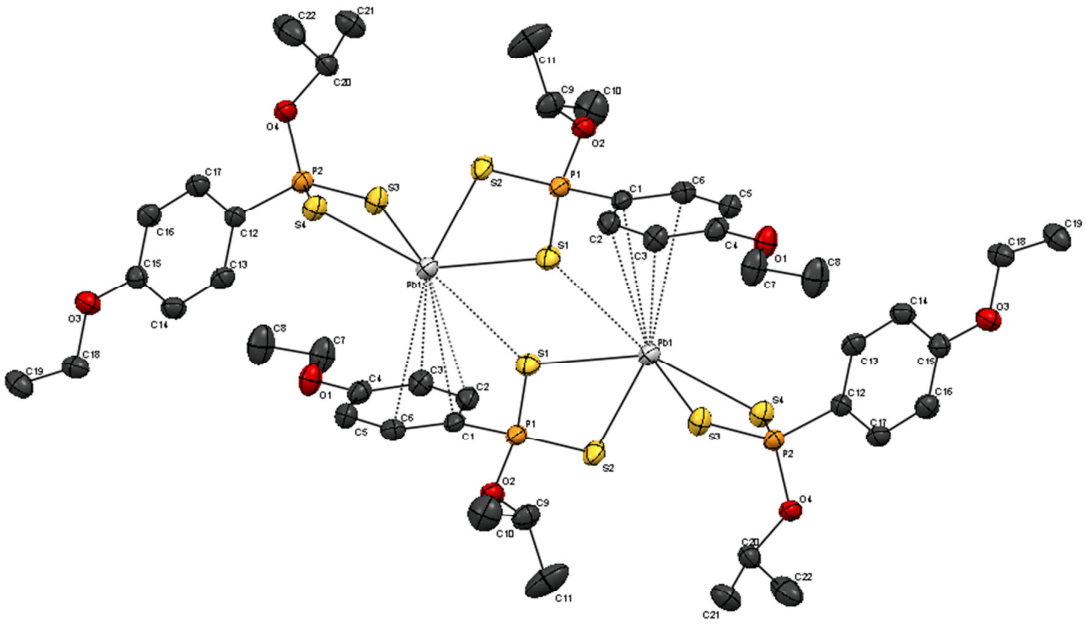

Figure 5.2: Dimeric pairs of complex 2D, comprised of intermolecular Pb···S and Pb···Ar interactions. Hydrogen atoms omitted for clarity.

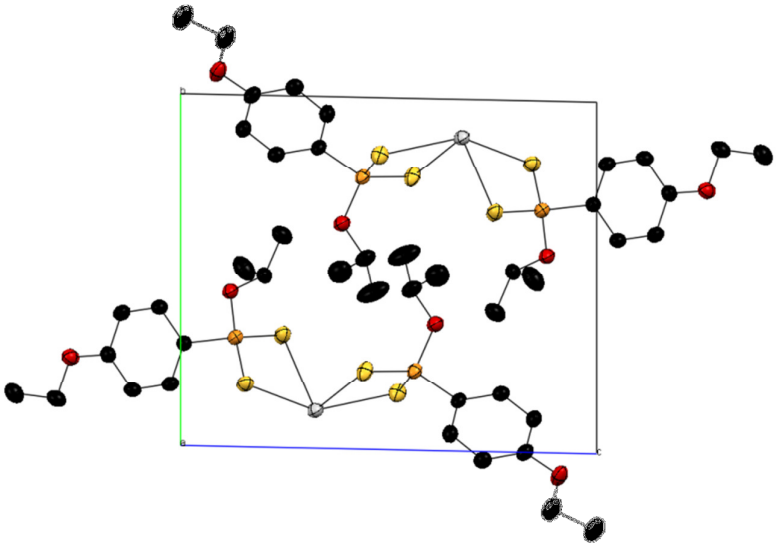

Figure 5.3: Crystallographic packing of 2D. Hydrogen atoms omitted for clarity.

Table 5.2: Crystal data and structure refinement for 2D

Empirical formula	C_{22} H_{32} O_4 P_2 Pb S_4
Formula weight	757.90
Temperature	173(2) K
Wavelength	0.71073
Crystal system	Triclinic
Space group	P-1
Unit cell dimensions	a = 10.2092(8) Å b = 11.7016(10)Å c = 12.9915(10)Å
	α =89.297(2)° β =85.016(2)° γ =69.0340(10)°
Volume	1443.5(2) $Å^3$
Z	2
Density (calculated)	1.744 Mg/m^3
Absorption coefficient	6.270
F(000)	744
Crystal size	0.11 x 0.14 x 0.16 mm^3
Theta range for data collection	1.57 to 28.38°
Index ranges	-13<=h<=13, -15<=k<=15, -17<=l<=17
Reflections collected	36710
Independent reflections	7212 [R(int) = 0.0366]
Completeness to theta	θ = 28.38° 99.4 %
Absorption correction	semi-empirical from equivalents
Max. and min. transmission	0.5455 and 0.4336
Refinement method	Full-matrix least-squares on F^2
Data / restraints / parameters	7212 / 0 / 304
Goodness-of-fit on F^2	1.032
Final R indices [I>2sigma(I)]	R1 = 0.0200, wR2 = 0.0441
R indices (all data)	R1 = 0.0245, wR2 = 0.0454
Largest diff. peak and hole	0.610 and -0.627 e.$Å^{-3}$

In summary this chapter discussed the formation, characterization and molecular structure of one new Pb(II) dithiophosphonato complex. The crystal structure is similar to one previous example reported in literature, being composed of dimeric pairs of distorted square pyramidal molecular units held together by intermolecular interactions.

5.4 References

1. I. P. Gray, A. M. Z. Slawin and J. D. Woollins, *Dalton Trans.*, 2004, 2477-2486.
2. I. P. Gray, H. L. Milton, A. M. Z. Slawin and J. D. Woollins, *Dalton Trans.*, 2003, 3450-3457.
3. S. Sewpersad and W. E. Van Zyl, *Acta Crystallogr., Sect. E: Struct.*, 2012, **68**, m1502.
4. H. Burzlaff and H. Zimmerman, International Union of Crystallography, 2006, vol. Volume A: Space Group Symmetry, pp. 818 - 820.
5. M. Karakus, H. Yilmaz and E. Bulak, *Russ. J. Coord. Chem.*, 2005, **31**, 316-321.

Chapter 6: Conclusions and Future Work

In this study, four new dithiophosphonate ligands were successfully synthesized from the reaction between simple aliphatic alcohols (methanol, 2-propanol, 1-propanol and 2-butanol), and the phenetole analogue of Lawesson's reagent. The study further prepared a number of new dithiophosphonate complexes, and they showed close comparisons with those in literature. In total, nine new complexes emerged from this study and their X-ray structures have been determined. The new complexes include four square planar Ni(II) complexes and a 6-coordinate Ni(II) adduct incorporating a 4-*tert*-butyl pyridine auxiliary ligand affording an octahedral Ni(II) complex. It also included three new dinuclear group 12 complexes, and one distorted pyramidal dimeric Pb(II) complex.

A number of structural comparisons of related structures within the study were made throughout. Comparisons were also made with other related structures previously reported and it was concluded that use of the phenetole analogue of Lawesson's reagent showed no significant structural differences when compared with regular Lawesson's reagent, except perhaps in the former case, some solubility issues in organic solvents were alleviated.

Future work

In this study, only complexes which rendered crystal structures were reported, whilst a host of other complexes were attempted but did not yield positive results. More group 11 metals (Cu, Ag, Au) ought to be attempted as they show different structural properties and introduce luminescent properties as well. Oxidation products of the ligand set should also be further examined since mild oxidizing agents such as I_2 could be used to generate disulfane compounds.

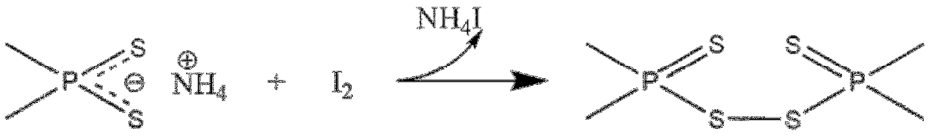

Scheme 6.1: Oxidation of a phosphor-1,1-dithiolate to a disulfane

Appendix

The accompanying CD serves as an Appendix to this dissertation and contains ^{31}P NMR, ^{1}H NMR, ^{13}C NMR and FTIR spectra and X-ray crystallographic data (including *cif* files).